TU Delft

BSc Thesis APPLIED MATHEMATICS

"Mathematical spatial compartmental epidemic models for the infectious disease cholera"

Eva van Tegelen
4725557

Delft University of Technology

Supervisor

Dr.ir. C. Vuik

Other members of the assessment committee

Dr.ir. M. Keijzer

...

Dr.ir. W.T. van Horssen

...

July, 2020

Delft

ABSTRACT

Cholera is an infectious disease caused by the bacterium *Vibrio cholerae*. Infections can occur directly via contact with infected people, but also indirectly via infected water. Because of these direct, but especially indirect infections, it is useful to investigate the spread of the disease using mathematical epidemic models. In this report a compartmental epidemic model for cholera is discussed: the SIRB model. This model consists of four compartments: susceptibles, infected, recovered and the bacterial concentration in water. The interaction between the groups is given by a system of differential equations. The equilibrium solutions and their stability are mathematically analysed. The main focus of this report, however, is on two different spatial models. The patches model consists of multiple patches connected by migration of people. Different measures against cholera are studied using this model. The second spatial model that has been numerically implemented is a diffusion SIRB model. The influence of the diffusion coefficients on the solution patterns will be researched for different initial conditions. The results presented in this report are building blocks for further research into compartmental models that simulate the spatial dynamics of cholera.

CONTENTS

Abstract **1**

List of Symbols **3**

List of Abbreviations **3**

1 Introduction **4**

2 Epidemic compartmental models **5**
2.1 SIR model 5
2.2 SIRB model 8

3 Mathematical analysis **13**
3.1 Reproduction number 13
3.2 Stability of the disease free equilibrium 14
3.3 Endemic equilibrium 17

4 Spatial SIRB patches model **19**
4.1 Derivation patches model 19
4.2 Influence of measures: Quarantine and Medicine 22
4.3 One reservoir 24
4.4 River 25
4.5 Discussion 27

5 Spatial SIRB diffusion model **28**
5.1 Derivation diffusion model 28
5.2 One point spread 28
5.3 Random spread 31
5.4 Discussion 33

6 Conclusion **34**

References **36**

A Finite difference matrix **37**

B Code SIRB model **38**

C Code Patches model **40**

D Code Diffusion model **44**

List of Symbols

Symbol	Description
S	Susceptibles
I	Infected
R	Recovered
B	Concentration of *V. cholerae* inside water
N	Total number of people inside the population
β_h	Human transmission number
γ	Recovery rate
μ	Mortality rate
Γ	Birth rate
β_e	Environmental transmission number
ϵ	Contamination rate from humans to water
g_b	Growth rate *V. cholerae* concentration in water
l_b	Loss rate *V. cholerae* concentration in water
K	Concentration *V. cholerae* at which chance of infection is 50%
$\lambda(B)$	Chance of getting infected by water with concentration B
R_0	Reproduction number
m_{ij}	Migration from patch j to patch i
D_1, D_2, D_3	Diffusion coefficients

List of Abbreviations

SIRB	Susceptibles, Infected, Recovered, Bacteria
DFE	Disease Free Equilibrium
EE	Endemic Equilibrium

1 INTRODUCTION

Cholera is an infectious disease caused by the bacterium *Vibrio cholerae*. Although there are more than two hundred different types of *V. cholerae*, there are two that can cause the disease in humans. [1] For most people a cholera infection is mild or without symptoms. However approximately 10% of infected will suffer more severe symptoms such as watery diarrhea, vomiting and leg cramps. [2] Humans can get infected by drinking infected water or eating food with the bacteria in it, but also by direct contact with infected feces. The source of infection of most epidemics is contamination of water or food by the feces of an infected individual. [2]

In some regions cholera remains a serious threat to public health. An estimation of the number of cases in the world is roughly 1.3 to 4.0 million a year. [3] Of all reported cases of cholera 54% occurred in Africa. A supply of safe water and sanitation is important to control the further spread of the disease.

To be able to control infectious diseases, such as cholera, it is critical to understand the transmission patterns of these diseases. Mathematical epidemiology is an important tool to study spread, but also to simulate the outcome of possible measures against an infectious disease. Compartmental models make the mathematical modelling simpler. The basic principle of compartmental modelling is the division of the population into multiple compartments, such as susceptibles and infected. The interaction between the different groups is then simulated using differential equations. Such deterministic epidemic models originate from the beginning of the 20th century. [4]

Since cholera is a disease where its primary source of infections is indirect contact, the disease is very interesting to study using mathematical compartmental models. Since the interactions between the different compartments such as the infected and susceptibles is not direct, adjustments have to be done to the basic compartmental model. Different cholera models have already been constructed and examined. [5][6][7][8] It is not only important to consider the total number of infected in a given region at a certain time, but also how the disease spreads itself within the region. To consider different measures against the infectious disease cholera, it is very useful to know how the infections will spread spatially. Such spatial compartmental disease models have already been widely created and studied for various diseases.[9][10][11]

The main objective of this research is to find and study a spatial compartmental model specific for the infectious disease cholera. In the first section the most basic compartmental model, the SIR model, will be discussed and extended into the specific cholera model being the SIRB model. In chapter 3 this SIRB model will be analysed mathematically by computing the reproduction number and by looking at the stability and existence of equilibriums. In the following chapters two spatial extensions of the SIRB model will be numerically implemented and discussed. The first spatial model in chapter 4 is made up of patches which are connected with each other by means of migration. Two different measures that could be taken to minimise the effects of a disease like cholera, quarantine and a medicine, are studied. The last model considered in chapter 5 is a diffusitive form of the SIRB model. Different initial infections and diffusion constants will be considered.

2 EPIDEMIC COMPARTMENTAL MODELS

Mathematical epidemic models can be used to investigate the spread of an infectious disease. A comparison of different measures can be performed to get better insight in how they might prevent further spreading in the population. Compartmental models are often used as a method to study the dynamics of these epidemics. In this chapter some of the simplest models for infectious diseases will be discussed.

2.1 SIR MODEL

One of the most basic compartmental models is the SIR model.[12] The assumption made in the SIR model is that a population can be divided into three groups: susceptibles, infectious and recovered. The susceptible part of the population consists of people that are still able to get the disease. When these people become infected they move to the infected group. From the infected it is possible to move to the recovered. For now it will be assumed that the recovered consist of people that have had the disease and that they are not able to get the disease again. The interactions between the three groups can also be seen in figure 2.1.

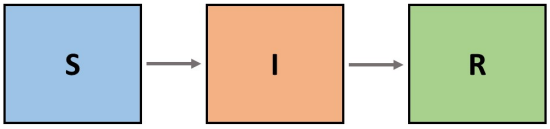

Figure 2.1: Visualisation of exchanges between the three groups of the SIR model (S=susceptibles, I=infected, R=recovered)

We will first study this SIR model without vital dynamics. This means that we leave out both births and deaths. The total population will therefore be constant. Without vital dynamics the model above can be described using the following differential equations:

$$\frac{dS}{dt} = -\frac{\beta_h IS}{N} \tag{2.1}$$

$$\frac{dI}{dt} = \frac{\beta_h IS}{N} - \gamma I \tag{2.2}$$

$$\frac{dR}{dt} = \gamma I \tag{2.3}$$

Here S are the susceptibles, I the infected and R the recovered. The total population is indicated by $N = S + I + R$ and is in this case constant. The parameter β_h is referred to as the transmission number. It depends on the number of contacts per individual per time unit and the probability of disease transmission between an infected and a susceptible. When we multiply this transmission number β_h with the number of susceptibles (S) and the fraction of infected in the entire population (I/N), the number of people that is moved from the susceptibles to the infected can be determined. These people are added to the group of infected and taken out of the susceptibles. From the infected compartment people that recover will cross to the recovered group R. The parameter γ is referred to as the recovery rate. The recovery rate indicates how fast people recover from the disease. When the average duration of an infectious disease is D, the recovery rate is $\gamma = \frac{1}{D}$.

The solution of this model can be approximated using for example an Euler Forward numerical scheme. In figure 2.2 a result of this model is shown. The model is presented for different values of the recovery rate γ and the transmission number β_h. At time $t = 0$ days the population

consists of 10 infected people and 1000 susceptibles. In the beginning no one has recovered from the infectious disease yet, so we have 0 recovered. The total population N is therefore 1010.

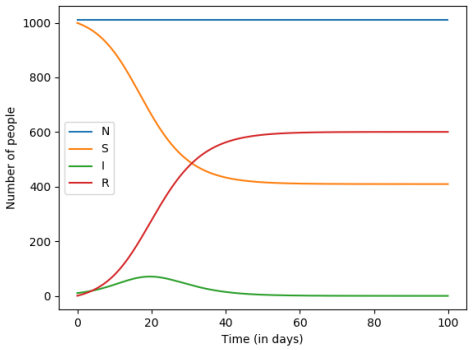

(a) $\gamma = \frac{1}{3}$ and $\beta = \frac{1}{2}$

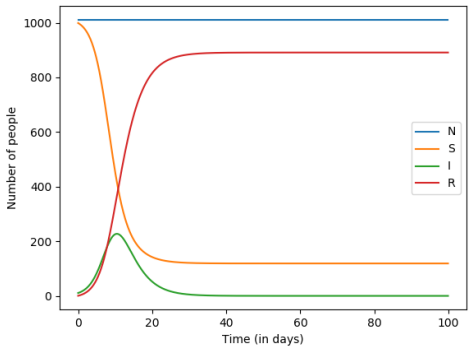

(b) $\gamma = \frac{1}{3}$ and $\beta_h = \frac{4}{5}$

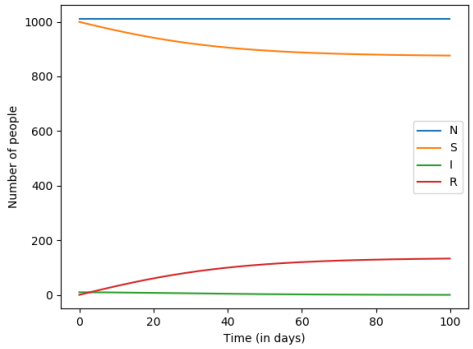

(c) $\gamma = \frac{1}{3}$ and $\beta_h = \frac{1}{3}$

Figure 2.2: SIR model using different values of γ and β_h over a period of 100 days

In figure 2.2a we find the decomposition of the population over a period of 100 days. For $\gamma = \frac{1}{3}$ and $\beta_h = \frac{1}{2}$ we indeed see an epidemic arising. After around 40 days the infected people have left the population, i.e. the population now only consists of susceptibles and recovered. We would expect that by increasing the transmission coefficient the epidemic will be larger as more people will get infected. This is indeed what we find in figure 2.2b. The peak in infected during the epidemic seems to occur earlier then in the previous model and is also higher. After 40 days the population is left with a larger group of recovered, than for the case of a lower transmission number. More people were infected by the disease. What happens if we choose a smaller transmission coefficient is illustrated in figure 2.2c. In this figure the number of infections does not peak as in in the other figures. Consequently a lot less people are infected.

Now the SIR model with vital dynamics will be considered. This will be done by taking into account deaths and births inside the population. When we take these into account, we obtain the following differential equations:

$$\frac{dS}{dt} = -\frac{\beta_h IS}{N} - \mu S + \Gamma N \tag{2.4}$$

$$\frac{dI}{dt} = \frac{\beta_h IS}{N} - \gamma I - \mu I \tag{2.5}$$

$$\frac{dR}{dt} = \gamma I - \mu R \tag{2.6}$$

We assume that a newborn inside the population is susceptible for the infectious disease. All babies that are born therefore enter the susceptible category. The birth rate Γ indicates the average amount of births per person per unit time inside the population. Furthermore we assume that in every category people die. For now we will assume that the mortality rate μ is the same in each of the groups. In reality this is often not true. A lot of infectious diseases can increase the chance of mortality. In figure 2.3 the results of the model are shown with and without vital dynamics.

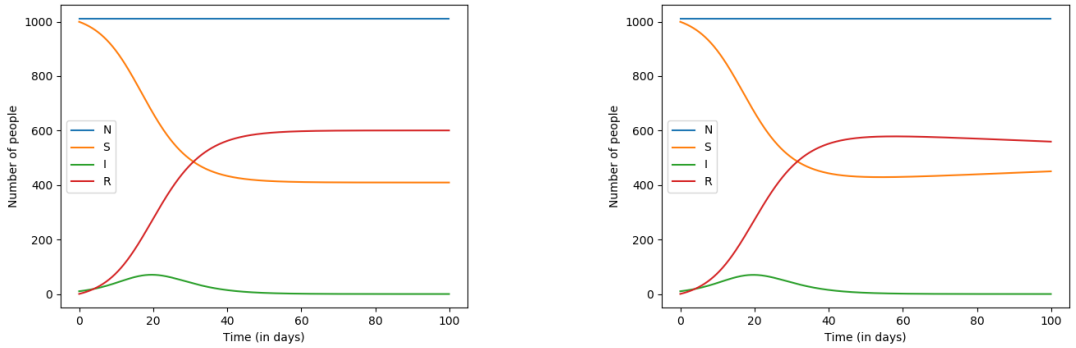

(a) $\gamma = \frac{1}{3}$ and $\beta = \frac{1}{2}$ without vital dynamics

(b) $\gamma = \frac{1}{3}$ and $\beta = \frac{1}{2}$ with vital dynamics

Figure 2.3: SIR model with and without vital dynamics over a period of 100 days, $\Gamma = \mu = 0.001$

In the solution showed above the mortality rate and the birth rate were taken equal ($\mu = \Gamma = 0.001$). This implies that every day 1.01 people die and are born in the population consisting op 1010 people. The total population size will stay the same, since each day the number of deaths is the same as the number of births. The models in figure 2.3 are similar when we compare the number of infected people during the epidemic. From 2.3b it can be seen that when vital dynamics are taken into account after around 45 days the number of recovered people starts descending. This makes sense as no new infections occur and the number of people that ever had the disease (recovered) becomes less due to mortality. At the same time this implies that the number of susceptible people starts increasing. Since the disease never leaves the population entirely, the increasing number of susceptibles might lead to a second wave of infections. In figure 2.4 this is illustrated.

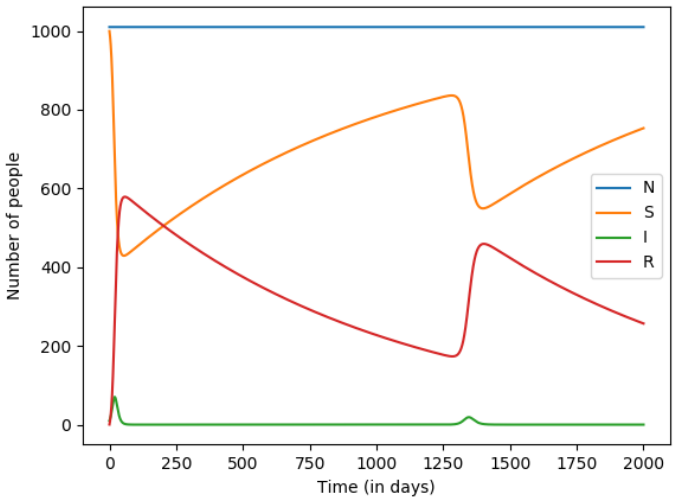

Figure 2.4: SIR model over a period of 2000 days with vital dynamics showing a second wave of the infectious disease, $\Gamma = \mu = 0.001$

Figure 2.4 shows the same solution as in 2.3b, but over a period of 2000 days. The first peak in infections is again at 20 days, but a second peak can be found after 1350 days (3.7 years). The number of infections is lower than during the first epidemic, since already more people are inside the recovered group and therefore will not be able to get the disease. In a model without vital dynamics a second wave of infections is not possible. The solution will reach an equilibrium where the number of susceptibles is constant.

In figure 2.5 the direction field of the solution of the SIR model is shown with and without vital dynamics. The right figure illustrates the same reoccurring peaks as figure 2.4. In figure 2.5a vital dynamics are left out and it can be concluded that the solution ends up in an equilibrium, after reaching a peak of 70 infected people. In figure 2.5b multiple infection waves can be seen. After each epidemic wave is over the number of susceptibles starts increasing again, creating a new wave. The number of infections during each wave becomes smaller.

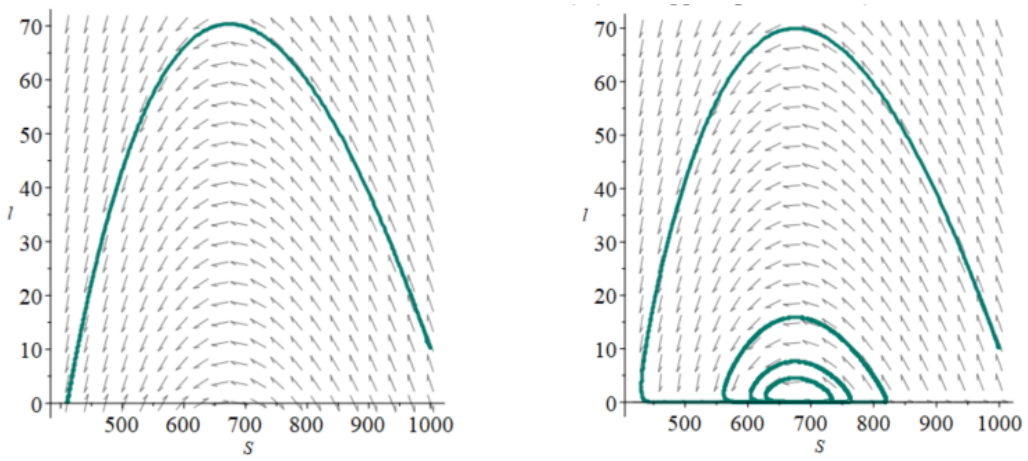

(a) $\gamma = \frac{1}{3}$ and $\beta = \frac{1}{2}$ without vital dynamics

(b) $\gamma = \frac{1}{3}$ and $\beta = \frac{1}{2}$ with vital dynamics

Figure 2.5: Direction field of the SIR model with and without vital dynamics, $\Gamma = \mu = 0.001$. On the horizontal axis: susceptibles (S). On the vertical axis: infected (I). The green line indicates the solution curve over time of the SIR models described in figure 2.3

The SIR model is one of the most basic and general mathematical epidemic models. It can reasonably predict the course of an infectious disease that is transmitted from humans to humans. This model can be extended to more disease specific models, such as for cholera.

2.2 SIRB MODEL

In this section we will examine a mathematical epidemic model more specific for cholera based on the research of Codeço et al.[6]. We will use the same parameter values as for the SIR model to compare the solutions of the different models. As mentioned before cholera is a bacterial disease that not only spreads from human to human, but can also spread via contact with infected water. In other words a big part of the infections does not happen through contact with another human being, but with the environment. In this section the SIR model will be further extended to the SIRB model which has an environmental aspect. In figure 2.6 the different groups that make up this model are shown. The interaction between the compartments is specified by means of arrows.

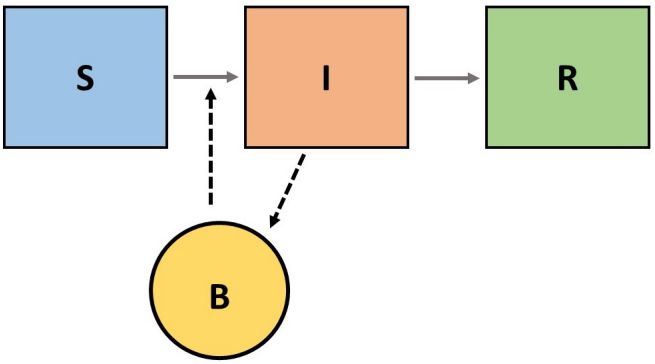

Figure 2.6: Visualisation of interactions between the four groups of the SIRB model (S=susceptibles, I=infectious, R=recovered, B=bacteria)

In figure 2.6 it can be seen that an extra group is added to the compartmental model. This group, the bacteria group, is the concentration of *V. cholerae* bacteria in the water. This group is not part of the population, but influences the dynamics between the other groups (indicated by the striped arrows). When we extend the SIR model with vital dynamics by adding this extra group, we gain the following system of four differential equations:

$$\frac{dS}{dt} = -\frac{\beta_h IS}{N} - \mu S + \Gamma N - \beta_e \lambda(B) S \tag{2.7}$$

$$\frac{dI}{dt} = \frac{\beta_h IS}{N} - \gamma I - \mu I + \beta_e \lambda(B) S \tag{2.8}$$

$$\frac{dR}{dt} = \gamma I - \mu R \tag{2.9}$$

$$\frac{dB}{dt} = \epsilon I + (g_b - l_b) B \tag{2.10}$$

From the first equation it can be seen that in comparison to the SIR model an additional term is added. This term indicates the number of susceptible people that get infected by the infectious water per unit time. The parameter β_e is the rate of exposure to the (contaminated) water. It shows how often susceptibles get in contact with the cholera infected water. The term $\lambda(B)$ is the probability of someone being infected by the water and logically depends on the bacteria concentration B in the water. In the paper of Codeço et al. the following equation for this term is suggested [6]:

$$\lambda(B) = \frac{B}{B+K} \tag{2.11}$$

where K is the concentration of the cholera bacteria in water for which the chance of susceptibles becoming infected is 50% when being in contact with the water. In figure 2.7 this relation between the probability of infection is represented against the bacteria concentration in the water for the value $K = 1000$. It illustrates that when the bacteria concentration in the water is already high (more than 1000), an even higher concentration has less effect on the probability of becoming infected, then when the concentration is low (less than 1000).

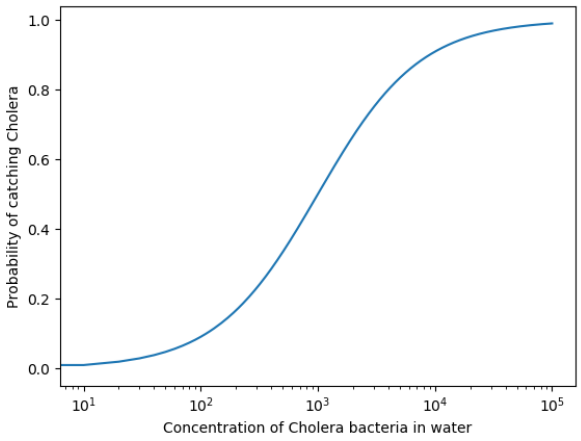

Figure 2.7: Probability of being infected against the concentration of *V. cholerae* in the water for $K = 1000$

The fourth equation 2.10 is the differential equation that describes the change in the bacteria concentration. The *V. cholerae* concentration in the water is influenced by infected people that come in contact with the water. The parameter ϵ indicates the influence of an infected individual on the bacteria concentration. Each time unit all infected people add the concentration ϵ to the bacteria group. The concentration of the cholera bacteria is additionally influenced by the growth and death of the bacterial population. The constant parameter g_b is referred to as the growth rate of the bacteria and l_b as the loss of the bacterial concentration. These differential equations can again be implemented using Euler Forward. The SIRB model will be compared to the SIR model of the previous section. The values of the parameters are stated in table 2.1. The values used are not realistic numbers and are taken unitless. They will be applied to show the properties of the SIRB model. For a realistic application of this model units and realistic numbers should be considered.

Parameter	Value
B_h	$\frac{1}{2}$
B_e	$\frac{1}{4}$
γ	$\frac{1}{3}$
μ	0.001
Γ	0.001
ϵ	1
g_b	0
l_b	0.1
K	1000

Table 2.1: Parameter values for the SIRB model

In the solution of figure 2.8 the same parameters are chosen as for the SIR model in figure 2.3. A clear difference can be seen between the solutions of the different models. Although the parameters for γ and β_h are chosen the same as for the SIR model, the number of infections is a lot bigger. This is mainly due to the additional influence of the environment. Because the number of infections is a lot bigger we end up with a population where the largest group is the recovered. The epidemic is also over faster, since after 20 days almost the entire population is recovered and therefore immune.

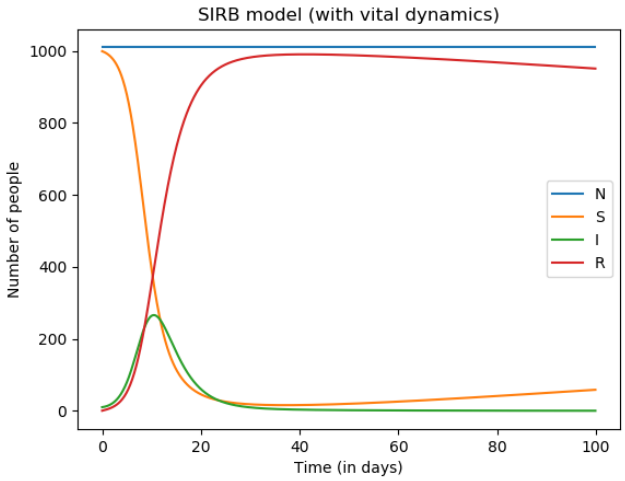

Figure 2.8: SIRB model over a period of 100 days using the parameters of table 2.1

In figure 2.9 the concentration of the cholera bacteria in the water corresponding to figure 2.8 is shown over the period of a 100 days. From the figure it appears that the bacterial concentration keeps increasing until day 20. After 20 days the influence of the infected people on the concentration becomes less than the dying of the bacteria. Therefore the bacterial concentration will start to decrease. The peak in the bacterial concentration occurs roughly at the same time as the peak of infections. This is in agreement with what would be expected. When there are a lot of infections inside the population, these infected people contribute more to the concentration of *V. cholerae* in the water.

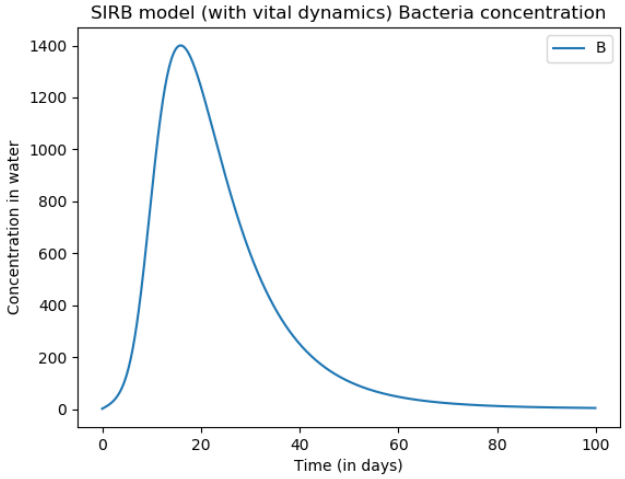

Figure 2.9: Bacterial concentration of the SIRB model using the parameters of table 2.1

A possible measure against the spreading of cholera is cleaning the water regularly. The concentration loss each time unit will be larger and the peak concentration will become a lot lower. In figure 2.10 the same solution as in figure 2.9 is shown, but with a higher dying ratio within the bacteria compartment. It can be seen that the peak of the bacteria concentration is a lot lower. If this result is compared with figure 2.7 it follows that the chance of catching the disease is a lot smaller for this concentration. The number of infections due to infected water and therefore the total infections will be smaller.

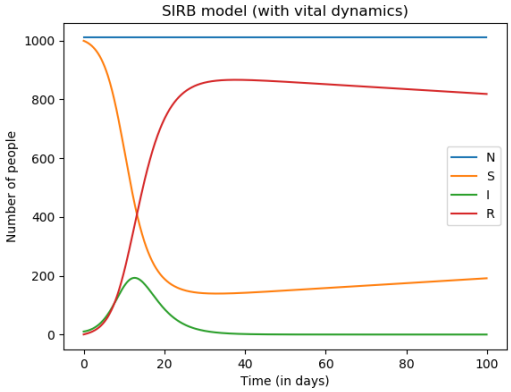

(a) Susceptibles,Infected,Recovered

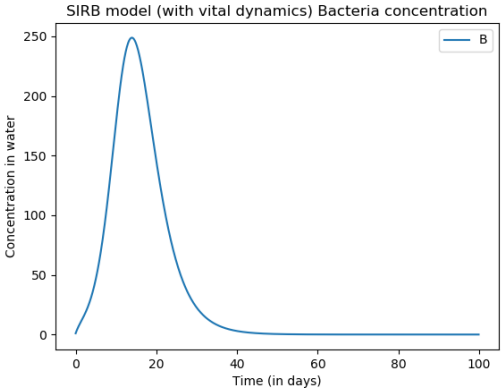

(b) Bacteria concentration

Figure 2.10: SIRB over a period of 100 days using $l_b = 0.75$

3 MATHEMATICAL ANALYSIS

To understand the behaviour of the SIRB model we will discuss some properties of the system of equations belonging to the model in this section. Different equilibrium solutions will be determined and studied.

3.1 REPRODUCTION NUMBER

Firstly the disease free equilibrium (DFE) will be calculated. As the name already suggests this equilibrium solution does not have any infected people and can be calculated by setting $\frac{dS}{dt} = \frac{dI}{dt} = \frac{dR}{dt} = \frac{dB}{dt} = 0$. The equilibrium values of the four different compartments will be denoted as S^o, I^o, R^o and B^o. Substituting $I^o = 0$ the following equilibrium can be determined:

$$DFE = (S^o, I^o, R^o, B^o) = (\frac{\Gamma N}{\mu}, 0, 0, 0) \tag{3.1}$$

This implies that if there are no infections and no bacteria in the environment, the population size will be constant and equal to S^o. Another very important property of an epidemic model is the basic reproduction number R_0. The basic reproduction number is defined as the expected number of secondary infections coming from an infected individual during the period where the person is infectious. This number is mostly used to see if a disease will spread through a population. If $R_0 < 1$ each infected person infects on average less than one susceptible person. The infected group will therefore become smaller and instinctively it would make sense if the disease would eventually leave the population. If $R_0 > 1$ the number of infected will increase and the disease will consequently take over a larger part of the population.

Using the method of Hoffernan et al. [13] and applying it to the model, similar as was done by van den Driessche et al. [14], the basic reproduction number can be calculated. According to Hoffernan et al. the reproduction number can be found by computing the largest eigenvalue of the next generation matrix FV^{-1} with F and V as follows assuming there are n compartments of which $1, ..., m$ are infected:

$$F = \left[\frac{\partial F_i(DFE)}{\partial x_j}\right] \qquad V = \left[\frac{\partial V_i(DFE)}{\partial x_j}\right] \tag{3.2}$$

with $i, j = 1, ..., m$ and where F_i is the appearance of new infections in compartment i and V_i is the rate of transfer of individuals to and from compartment i. These matrices have to be analysed at the disease free equilibrium (DFE), which has just been determined. Applying this to our SIRB model, similarly as done by van den Driessche et al., the following matrices are obtained:

$$F = \begin{bmatrix} \frac{\beta_h \Gamma}{\mu} & \frac{\beta_e \Gamma N}{\mu k} \\ 0 & 0 \end{bmatrix} \qquad V = \begin{bmatrix} \mu + \gamma & 0 \\ -\epsilon & -(l_b - g_b) \end{bmatrix} \tag{3.3}$$

Here the growth of bacteria has not been taken as a form of new infections, so it does not appear in matrix F. Taking the inverse of V and multiplying both matrices the next generation matrix can be gained:

$$FV^-1 = \begin{bmatrix} \frac{\Gamma \beta_h}{\mu(\mu+\gamma)} + \frac{\epsilon \Gamma N \beta_e}{k\mu(\mu+\gamma)(l_b - g_b)} & \frac{\Gamma N \beta_e}{\mu k(l_b - g_b)} \\ 0 & 0 \end{bmatrix} \tag{3.4}$$

By taking the largest eigenvalue the reproduction number R_0 is obtained, which can be divided into human and bacterial infections, as can be seen below:

$$\begin{aligned} R_0 &= R_0^h + R_0^e \\ &= \frac{\Gamma N \beta_h}{\mu(\mu+\gamma)N} + \frac{\epsilon \Gamma N \beta_e}{k\mu(\mu+\gamma)(l_b - g_b)} \end{aligned} \tag{3.5}$$

We will now examine two cases to study the influence of the reproduction number on the solution of the model. In figure 3.1 two solutions of SIRB models are presented using different parameters. The figure shows that for the reproduction number less than one no real peak in infections can be seen. Although still a part of the population gets infected, the number of infections is significantly lower than in figure 3.1b.

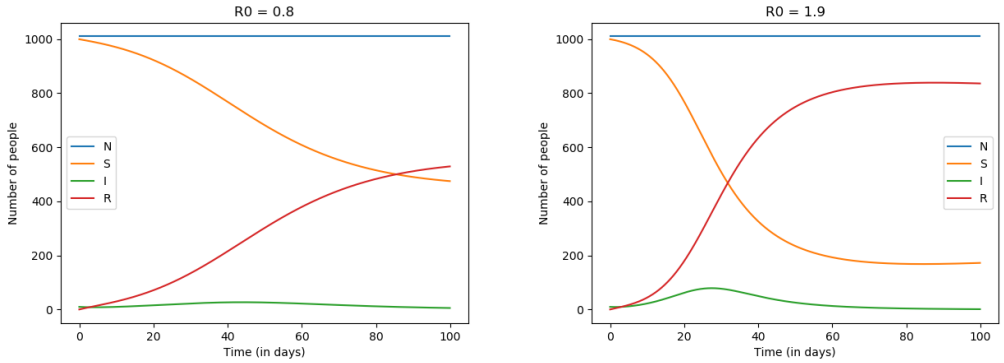

(a) $R_0 = 0.8$ (b) $R_0 = 1.9$

Figure 3.1: SIRB over a period of 100 days for different reproduction numbers R_0

If we look at the long term solutions of these models described in figure 3.1 another difference can be noted. In figure 3.2 these models are shown over a period of 8000 days. It can be seen that the groups inside the model go to an equilibrium solution. It illustrates that for a higher reproduction number the equilibrium solution of susceptibles is lower, than for a small reproduction number. This makes sense as more people get infected.

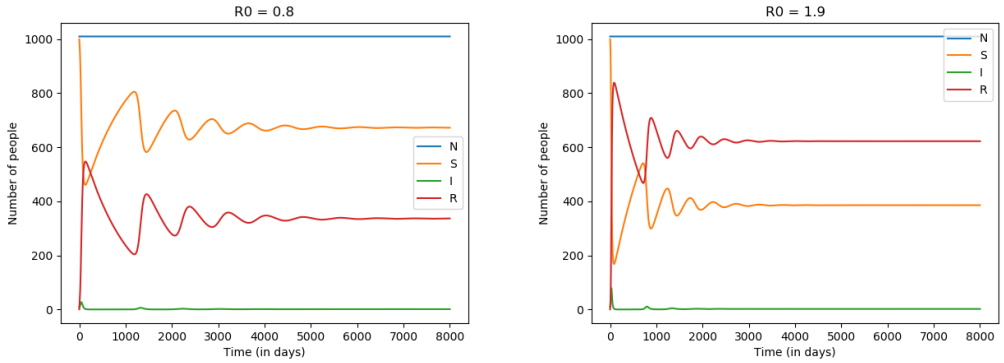

(a) $R_0 = 0.8$ (b) $R_0 = 1.9$

Figure 3.2: SIRB over a period of 8000 days for different reproduction numbers R_0

3.2 Stability of the disease free equilibrium

To study the stability of the disease free equilibrium the Jacobian matrix will be determined and evaluated at (S^o, I^o, R^o, B^o). For now it will be assumed that the population size N is fixed. This also means that the mortality rate must equal the birth rate ($\mu = \Gamma$). From equations (2.7-2.10) the following Jacobian matrix is obtained:

$$J = \begin{bmatrix} \frac{-\beta_h I}{N} - \mu - \beta_h \frac{B}{B+k} & \frac{-\beta_h S}{N} & -\beta_e \frac{k}{(B+k)^2} S \\ \frac{\beta_h I}{N} + \beta_h \frac{B}{B+k} & \frac{\beta_h S}{N} - \gamma - \mu & \beta_e \frac{k}{(B+k)^2} S \\ 0 & \epsilon & g_b - l_b \end{bmatrix} \tag{3.6}$$

Substituting in the disease free equilibrium we get:

$$J(DFE) = \begin{bmatrix} -\mu & -\beta_h & -\beta_e \frac{N}{k} \\ 0 & \beta_h - \gamma - \mu & \beta_e \frac{N}{k} \\ 0 & \epsilon & g_b - l_b \end{bmatrix} \tag{3.7}$$

The equilibrium solution is stable if the real part of the eigenvalues of this matrix are all smaller than zero. A method of bounding the eigenvalues is Gershgorin's circle theorem. Applying this theorem to our matrix we obtain three bounds for the eigenvalues λ_i of this matrix:

$$-\beta_h - \beta_e \frac{N}{k} - \mu \leq \lambda_i \leq \beta_h + \beta_e \frac{N}{k} - \mu \tag{3.8}$$

$$-\beta_e \frac{N}{k} + \beta_h - \gamma - \mu \leq \lambda_i \leq \beta_h \frac{N}{k} + \beta_h - \gamma - \mu \tag{3.9}$$

$$-\epsilon + g_b - l_b \leq \lambda_i \leq \epsilon + g_b - l_b \tag{3.10}$$

For all parameter values where the upper bounds of these eigenvalues are smaller than zero the DFE is guaranteed stable. However, simulations show that also for some parameters values for which the upper right bound is larger than zero the equilibrium solution is still stable. Although part of the Gershgorian disks lies in the right half of the imaginary plane, it does not necessarily imply that there must be eigenvalues with real part larger than zero. To say more about the general stability we need to consider a different method.

By studying the characteristic polynomial it can be seen that one of the eigenvalues is $\lambda_1 = -\mu$, which is always negative. When this eigenvalue is divided out, the following characteristic polynomial is left for the remaining eigenvalues:

$$\lambda^2 - (\beta_h - \gamma - \mu + g_b - l_b)\lambda + (\beta_h - \gamma - \mu)(g_b - l_b) - \epsilon\beta_e \frac{N}{k} = 0 \tag{3.11}$$

For this characteristic polynomial a Routh table can be constructed [15]:

1	$(\beta_h - \gamma - \mu)(g_b - l_b) - \epsilon\beta_e \frac{N}{k}$
$-(\beta_h - \gamma - \mu + g_b - l_b)$	0
$(\beta_h - \gamma - \mu)(g_b - l_b) - \epsilon\beta_e \frac{N}{k}$	

Table 3.1: Routh table for equation 3.11

According to Routh's theorem all zeroes of the characteristic polynomial have negative real part and imaginary part nonzero if and only if all entries in the first column have the same sign. So we obtain two new bounds for the parameter values that imply a stable disease free equilibrium.

$$-\beta_h + \gamma + \mu - g_b + l_b > 0 \tag{3.12}$$

$$(\beta_h - \gamma - \mu)(g_b - l_b) - \epsilon\beta_e \frac{N}{k} > 0 \tag{3.13}$$

Still this bound does not cover all stable parameter values. Eigenvalues which have negative real part and zero imaginary part are also stable, but are not considered using Routh's theorem.

To be sure that all stable eigenvalues are found we compute the eigenvalues and check for which parameters these are stable. For a general 2x2 matrix A we obtain the following eigenvalues:

$$A = \begin{bmatrix} a & b \\ c & d \end{bmatrix} \qquad \lambda_i = \frac{a+d}{2} \pm \frac{\sqrt{(a-d)^2 + 4bc}}{2} \tag{3.14}$$

Since we already found a bound for imaginary eigenvalues we will focus on real eigenvalues only. For stability all eigenvalues need to be negative, so it is enough to study the largest eigenvalue and bound it by zero:

$$\frac{a+d}{2} + \frac{\sqrt{(a-d)^2+4bc}}{2} < 0 \tag{3.15}$$

$$\sqrt{(a-d)^2+4bc} < -(a+d) \tag{3.16}$$

Since we considered this to be the largest eigenvalue we at least need $(a+d) < 0$ for the eigenvalue to be negative. Squaring both sides we then obtain:

$$(a-d)^2 + 4bc < (a+d)^2 \tag{3.17}$$

$$a^2 + d^2 - 2ad + 4bc < a^2 + d^2 + 2ad \tag{3.18}$$

$$4(bc-ad) < 0 \tag{3.19}$$

$$ad - bc > 0 \tag{3.20}$$

Stability of a 2x2 matrix is therefore guaranteed if the following three properties hold:

1. $(a-d)^2 + 4bc > 0$
2. $a + d < 0$
3. $ad - bc > 0$

Substituting the values of our matrix we obtain the following criteria:

1. $(\beta_h - \gamma - \mu - g_b + l_b)^2 + 4\epsilon\beta_e \frac{N}{k} > 0$
2. $\beta_h - \gamma - \mu + g_b - l_b < 0$
3. $(\beta_h - \gamma - \mu)(g_b - l_b) - \epsilon\beta_e \frac{N}{k} > 0$

This last property can be connected to the reproduction number R_0. Since the mortality rate was taken equal to the birth rate, we have the following reproduction number:

$$R_0 = \frac{\beta_h}{\mu+\gamma} + \beta_e \epsilon \frac{N}{k} \frac{1}{(\mu+\gamma)(l_b - g_b)} \tag{3.21}$$

This R_0 can be substituted into the third property and the following inequality is obtained assuming that $(g_b - l_b) < 0$:

$$(\beta_h - \gamma - \mu)(g_b - l_b) + (R_0(\mu+\gamma) - \beta_h)(g_b - l_b) > 0 \tag{3.22}$$

$$-\gamma - \mu + R_0(\mu+\gamma) < 0 \tag{3.23}$$

$$(R_0 - 1)(\mu+\gamma) < 0 \tag{3.24}$$

$$R_0 < 1 \tag{3.25}$$

So it turns out that if the reproduction number R_0 is smaller than one the DFE is stable. This is in agreement with the intuition that for a reproduction number smaller than one, the number of infections will decrease. When there is a small disturbance around the disease free equilibrium the solution will again converge to an equilibrium of zero infected. When R_0 is larger than one, the third property is not satisfied. A small disturbance will than lead to a further increase of infected away from the disease free equilibrium. The equilibrium is unstable.

3.3 ENDEMIC EQUILIBRIUM

Not all solutions reach an equilibrium where the number of infected people is zero. Such a non-zero equilibrium is called the endemic equilibrium (EE) and can be calculated by setting $\frac{dS}{dt} = \frac{dI}{dt} = \frac{dR}{dt} = \frac{dB}{dt} = 0$. Again it is assumed that the total population N is constant. The endemic equilibrium will be denoted by (S^*, I^*, B^*). Substituting this notation and setting the derivatives equal to zero we obtain the following system of equations.

$$\frac{dS^*}{dt} = -\frac{\beta_h I^* S^*}{N} - \mu S^* + \Gamma N - \beta_e \lambda(B^*) S = 0 \tag{3.26}$$

$$\frac{dI^*}{dt} = \frac{\beta_h I^* S^*}{N} - \gamma I^* - \mu I^* + \beta_e \lambda(B^*) S = 0 \tag{3.27}$$

$$\frac{dB^*}{dt} = \epsilon I^* + (g_b - l_b) B^* = 0 \tag{3.28}$$

Expressing B^* and S^* in terms of I^* the following expressions can be derived:

$$B^* = \frac{\epsilon I^*}{l_b - g_b} \qquad S^* = \frac{\Gamma N}{\mu} - \frac{(\mu+\gamma) I^*}{\mu} \tag{3.29}$$

Substituting these both inside the second equation, the following equation is gained:

$$\frac{\beta_h}{N} I^* (\frac{\Gamma N}{\mu} - \frac{(\mu+\gamma)}{\mu} I^*) - \gamma I^* - \mu I^* + \beta_h \frac{\epsilon I^*}{\epsilon I^* + k(l_b - g_b)} (\frac{\Gamma N}{\mu} - \frac{(\mu+\gamma)}{\mu} I^*) = 0 \tag{3.30}$$

Dividing this equation once by I^*, which gives us the solution of the disease free equilibrium $I^o = 0$, this equation can be written as a quadratic equation of the form:

$$p_2 I^{*2} + p_1 I^* + p_0 = 0 \tag{3.31}$$

with

$$p_0 = k(l_b - g_b)(\Gamma \beta_h - \mu(\mu+\gamma)) + \epsilon N \Gamma \beta_e \tag{3.32}$$

$$p_1 = -(l_b - g_b) k \frac{\beta_h}{N} (\mu+\gamma) + \epsilon(\Gamma \beta_h - \mu(\mu+\gamma)) - \beta_e \epsilon(\mu+\gamma) \tag{3.33}$$

$$p_2 = -\epsilon \frac{\beta_h}{N} (\mu+\gamma) \tag{3.34}$$

The positive non-zero solutions of this equation give the endemic equilibrium I^*. These zeroes can be calculated using known formulas. Moreover, it can be studied under which circumstances this quadratic equation has such a positive non-zero solution. We know that the two zeroes I_1^* and I_2^* of the quadratic equation 3.31 must satisfy:

$$I_1^* I_2^* = \frac{p_0}{p_2} \tag{3.35}$$

$$I_1^* + I_2^* = -\frac{p_1}{p_2} \tag{3.36}$$

Firstly note that p_2 is always negative, since all parameters in the equation are larger than zero. Two cases will be considered to study the existence of a positive non-zero solution:

- $R_0 > 1$:
  Using the reproduction number of equation 3.5 we get the following:

$$\frac{\Gamma \beta_h}{\mu(\mu+\gamma)} + \frac{\epsilon \Gamma N \beta_e}{k\mu(\mu+\gamma)(l_b - g_b)} > 1 \tag{3.37}$$

$$\beta_h \Gamma k(l_b - g_b) + \beta_e \epsilon N \Gamma - k\mu(\mu+\gamma)(l_b - g_b) > 0 \tag{3.38}$$

$$p_0 > 0 \tag{3.39}$$

  Since $p_0 > 0$ and $p_2 < 0$ equation 3.35 implies that $I_1^* I_2^* < 0$. This entails that one of the zeroes is positive and non-zero. So if $R_0 > 1$ the non-zero endemic equilibrium exists.

- $R_0 < 1$:
  Using the same reasoning as above we obtain that $p_0 < 0$ when $R_0 < 1$. This implies that $I_1^* I_2^* > 0$. So we can conclude that either $I_1^*, I_2^* > 0$ or $I_1^*, I_2^* < 0$. We again consider the reproduction number:

$$\frac{\Gamma\beta_h}{\mu(\mu+\gamma)} + \frac{\epsilon\Gamma N\beta_e}{k\mu(\mu+\gamma)(l_b-g_b)} < 1 \tag{3.40}$$

  Suppose $l_b > g_b$, then it must be true that

$$\frac{\Gamma\beta_h}{\mu(\mu+\gamma)} < 1 \quad \text{and} \quad \frac{\epsilon\Gamma N\beta_e}{k\mu(\mu+\gamma)(l_b-g_b)} < 1 \tag{3.41}$$

  If we now take a closer look at p_1 and use one of the inequalities above we get the following:

$$p_1 = -(l_b-g_b)k\frac{\beta_h}{N}(\mu+\gamma) + \epsilon(\Gamma\beta_h - \mu(\mu+\gamma)) - \beta_e\epsilon(\mu+\gamma) \tag{3.42}$$

$$\frac{p_1}{(\mu+\gamma)\mu} = -(l_b-g_b)k\frac{\beta_h}{N\mu} + \frac{\epsilon\Gamma\beta_h}{(\mu+\gamma)\mu} - \epsilon - \frac{\beta_e\epsilon}{\mu} \tag{3.43}$$

  Now applying the left equality of equation 3.41 we obtain that

$$\frac{p_1}{(\mu+\gamma)\mu} < -(l_b-g_b)k\frac{\beta_h}{N\mu} + \epsilon - \epsilon - \frac{\beta_e\epsilon}{\mu} \tag{3.44}$$

$$= -(l_b-g_b)k\frac{\beta_h}{N\mu} - \frac{\beta_e\epsilon}{\mu} \tag{3.45}$$

$$< 0 \tag{3.46}$$

  Since $\mu(\mu+\gamma) > 0$ we can conclude that if $R_0 < 1$ and $l_b > g_b$ we have that $p_1 < 0$. Using this and equation 3.36 it can be seen that $I_1^* + I_2^* < 0$. This implies that both I_1^* and I_2^* are negative. Therefore if $R_0 < 1$ there exists no non-zero endemic equilibrium.

So an endemic equilibrium only exists for $R_0 > 1$. For $R_0 < 1$ the solution will always go to the disease free equilibrium, where the number of infected people is zero.

4 SPATIAL SIRB PATCHES MODEL

So far no spatial aspect was added to the SIRB model. In this section we will consider a spatial extension of the model by looking at different patches.[16] This method was earlier applied by Arino et al. to a different epidemic model (SEIRS)[17] and by Eisenberg et al. to a similar cholera model [18]. In this section it will be applied to our SIRB model.

4.1 DERIVATION PATCHES MODEL

This model expansion consists of a population divided over n patches. Each patch $p = 1, ..., n$ has its own population of susceptibles (S_p), infected (I_p) and recovered (R_p). The entire population in patch p is given by $N_p = I_p + S_p + R_p$. Furthermore it is possible that travel or migration occurs between the different patches. Moreover it is assumed that each patch has its own water reservoir where the bacterial concentration is denoted by B_p. The population size inside a patch can change due to mortality and birth, but also due to travel. The difference in population size inside a patch p due to travel to and from other patches denoted by N'_p is given by:

$$N'_p = \sum_{q=1}^{n} (m_{pq}N_q - m_{qp}N_p) \tag{4.1}$$

where m_{pq} denotes the travel/migration rate from patch q to patch p. If we combine the migration term determined above with the single compartmental SIRB model the following system is obtained for each of the patches $p = 1, ..., n$:

$$\frac{dS_p}{dt} = -\frac{\beta_{hp} I_p S_p}{N_p} - \mu_p S_p + \Gamma_p N_p - \beta_{ep}\lambda(B_p)S_p + \sum_{q=1}^{n} (m_{pq}S_q - m_{qp}S_p) \tag{4.2}$$

$$\frac{dI_p}{dt} = \frac{\beta_{hp} I_p S_p}{N_p} - \gamma_p I_p - \mu_p I_p + \beta_{ep}\lambda(B_p)S_p + \sum_{q=1}^{n} (m_{pq}I_q - m_{qp}I_p) \tag{4.3}$$

$$\frac{dR_p}{dt} = \gamma_p I_p - \mu_p R_p + \sum_{q=1}^{n} (m_{pq}R_q - m_{qp}R_p) \tag{4.4}$$

$$\frac{dB_p}{dt} = \epsilon_p I_p + (g_{bp} - l_{bp})B_p \tag{4.5}$$

where the parameters β_{hp}, β_{ep}, μ_p, Γ_p, γ_p, ϵ_p, g_{bp} and l_{bp} are the same as described in the previous section, but can now be patch dependent. Multiple patch structures can be considered. We will first investigate matrix like patch structures and later on ring structures. In figure 4.1 the interaction between the patches due to travel/migration is shown. Each patch can only interact with adjacent patches.

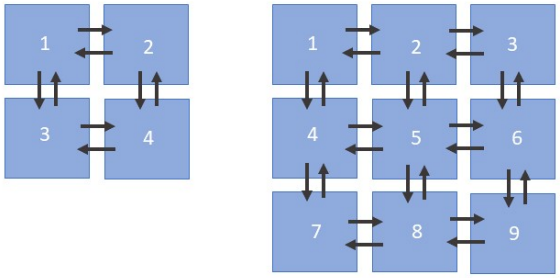

Figure 4.1: Matrix structure migration between the patches shown for $n = 4$ and $n = 9$ patches

This model has been simulated for 4 and 9 patches. The parameters β_h, β_e, μ, Γ, γ, ϵ, g_b and l_b were taken equal on each patch with the values described in 2.1. The migration rate between two adjacent patches p and q is given by m_{pq} and is taken the same between all adjacent patches. The initial values at $t = 0$ for the different population groups inside the patches are given by $S_p(0) = 1000$, $I_p(0) = 0$, $R_p(0) = 0$ and $B_p(0) = 0$ for $p = 2, ..., n$. Only in the first patch cholera infected people occur. The initial conditions for $p = 1$ are $S_p(0) = 1000$, $I_p(0) = 10$, $R_p(0) = 0$ and $B_p(0) = 0$. In figure 4.2 the solution of the number of infected in each patch is shown.

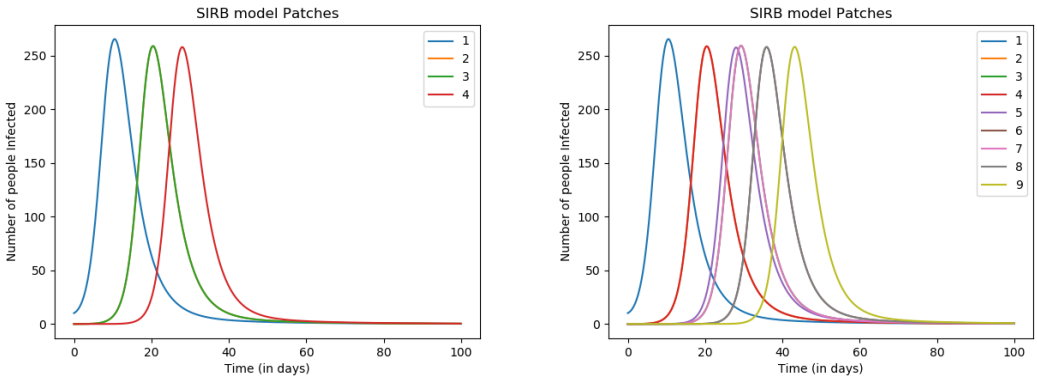

(a) 4 patches

(b) 9 patches

Figure 4.2: Number of infected people over a period of 100 days for the SIRB patches model for $m_{pq} = 0.001$ (matrix structure)

In figure 4.2a it can be seen that the first peak happens in patch $p = 1$. Since this patch was the only patch with infections as initial value this makes sense. The following peaks (a little lower) happen in patch $p = 2$ and $p = 3$. These are the adjacent patches to the patch were the first epidemic occurred, so again this agrees with what one would expect. The patch with the furthest distance from the infection origin reaches a peak latest. The same can be seen in figure 4.2b if we look at a bigger patch structure. Now patch $p = 2$ and $p = 4$ are the adjacent patches to the first patch and therefore will be the first to also reach an epidemic. When more migration takes place the infections between the patches will happen earlier, since infected people will sooner reach the not yet infected patches. This is exactly what can be seen in figure 4.3 below.

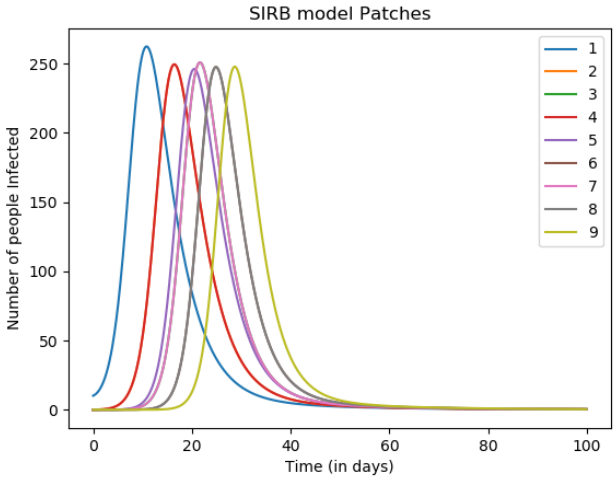

Figure 4.3: Number of infected people over a period over 100 days for $m_{pq} = 0.01$ (matrix structure)

Figure 4.3 illustrates that the epidemic waves in each of the patches happen sooner after each other when there is more travel. The migration rate between the patches is ten times larger and therefore also the exchange of infected people. By changing the migration rate the influence of different measures, such as quarantine, can be considered. This will be done later in this section. Another interesting patch structure is the ring structure shown in figure 4.4 below. We will consider two possibilities: one way traffic and two way traffic. In the figure one way traffic is indicated by the black arrows. People from patch p can only travel to patch $p+1$ or when $p = n$ to patch 0. When two way traffic is considered the green arrows are also taken into account. So additional to the travel described above, people from patch p can also travel to patch $p-1$.

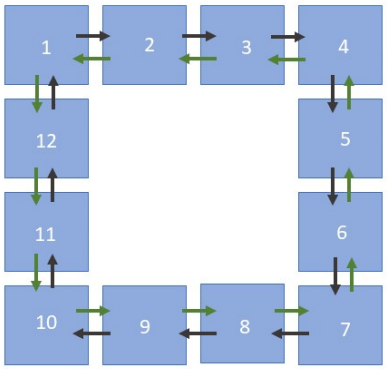

Figure 4.4: Ring structure migration between the patches shown for $n = 12$ patches

Both the one way and two way ring structures were implemented using the same parameters as in figure 4.2. The number of infected people in each of the ring structures can be seen in figure 4.5. One of the first things that catches the eye is the difference in shape of spread. In figure 4.5a patch $p = 10$ is the last patch to obtain the peak. The patch is furthest away from the initial source and consequently last reached by migrating infected people. It will therefore be the last patch to experience an epidemic. When two way traffic is considered patch $p = 10$ is after patch 1 the first patch to have a peak in infections. With two way traffic that patch is the first to be reached due to infected migration and patch $p = 6$ will be last reached as also can be seen in the figure. This explains the difference in shape of spread between the patches for one and two way traffic.

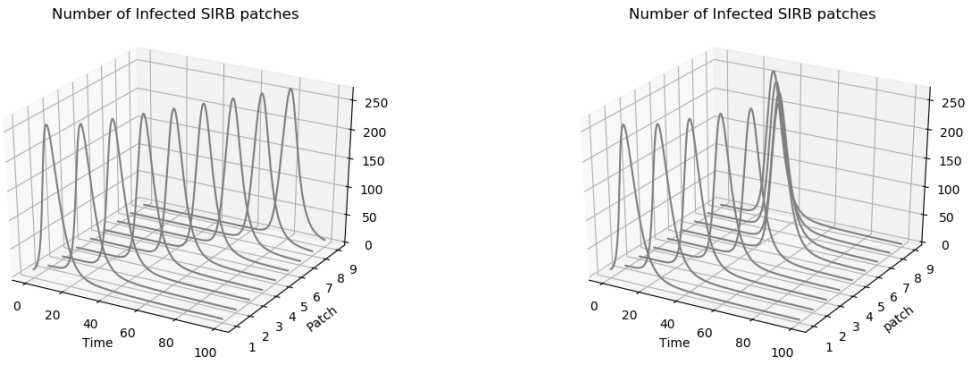

(a) One way traffic

(b) Two way traffic

Figure 4.5: Number of infected people over a period of 100 days for the SIRB patches model for $m_{pq} = 0.001$ (ring structure using 10 patches)

The model has also been implemented for a large number of patches. In figure 4.6 the number of infected people are shown at the different patches. To better represent the spreading of the disease the different are patches are plotted and the darker the colour the more infected people that patch includes. The initial infection is in patch 113 and examining the figures it can be seen that the infections spread outwards due to migration.

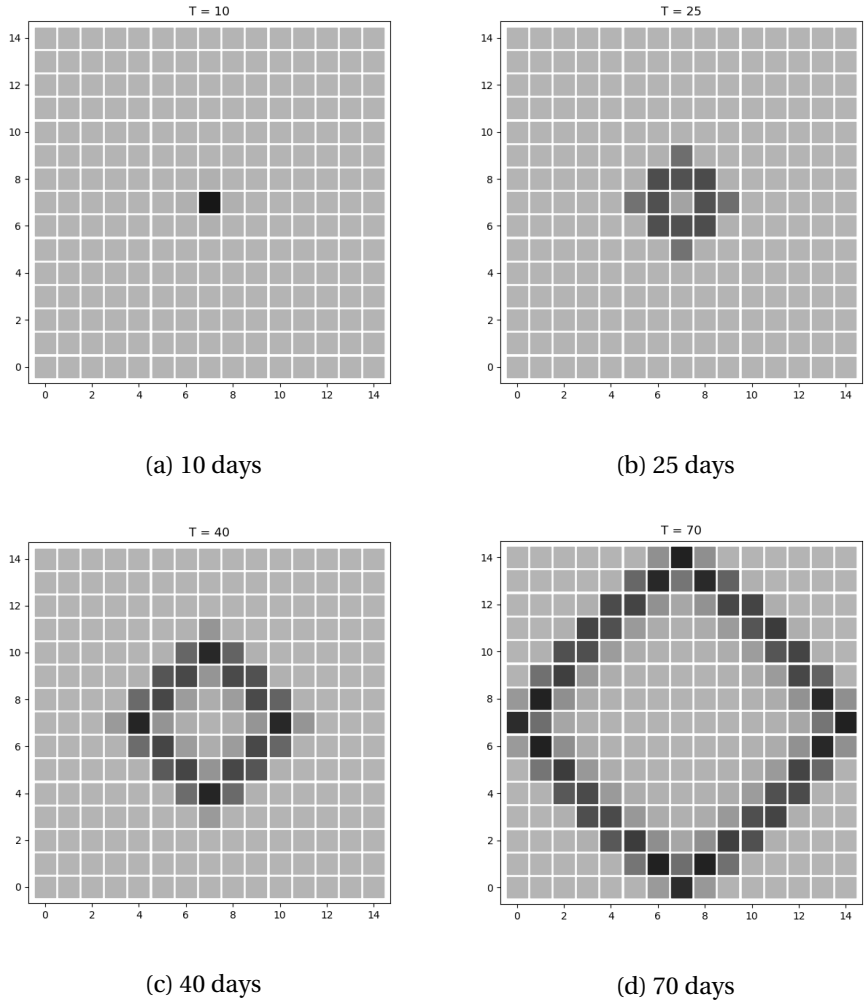

(a) 10 days

(b) 25 days

(c) 40 days

(d) 70 days

Figure 4.6: Number of infected people at multiple time instances for the SIRB patches model for $m_{pq} = 0.001$ (matrix structure $15x15$). Initial infection at patch 113

4.2 Influence of measures: Quarantine and Medicine

Using this large number of patches we will consider two different solutions that possibly minimise epidemics: quarantine and medicine. When a patch goes into quarantine it means that no migration with other patches occurs. It will be assumed that a patch goes into quarantine if it has reached a minimal number of infections. Since creating a new medicine takes time, we will assume that a medicine is available after a certain amount of days (30 days in our implementation) and that it will increase the recovery rate. In other words, people will recover sooner from the disease and will move faster from the infectious to the recovered. In figure 4.7 these measures are compared to the original infection spread.

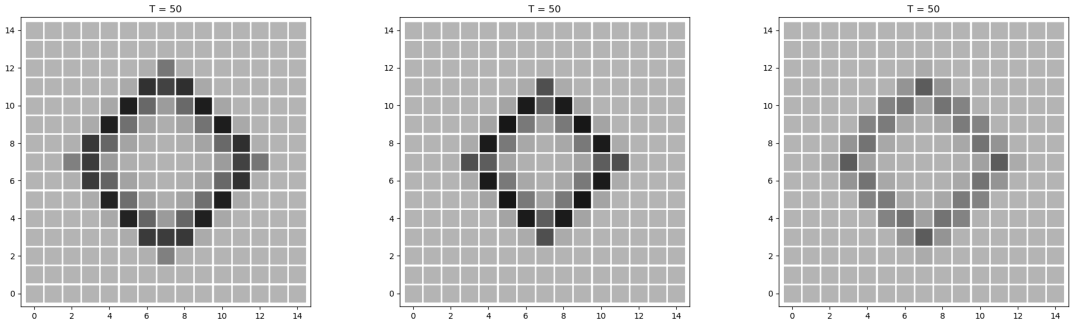

(a) No measure (b) Quarantine at $I_p = 10$ (c) Medicine after 30 days

Figure 4.7: Number of infected people after 50 days for the SIRB patches model for $m_{pq} = 0.001$ (matrix structure $15x15$). Initial infection at patch 113.

In figure 4.7b we can see that the number of infections with quarantine is not necessarily lower than when no measures are taken, but we can see that the infectious disease spreads slower between the patches. This agrees with what we would expect. It was assumed that a patch goes into quarantine if the number of infected is larger than 10. If the number of infections becomes lower the quarantine is over and migration starts again. These infections than are still able to reach nearby patches, but it goes slower than when no measures are taken.

In figure 4.7c the number of infections is shown when after 30 days a medicine is available that shortens the average duration of the disease from 3 days ($\gamma = \frac{1}{3}$) to 2 days ($\gamma = \frac{1}{2}$). It can be seen that the number of infections is significantly smaller than when no measures are taken. The spread between patches also goes a little slower. Since the number of infections in the patches is lower, also the migration of infected individuals is less. It therefore takes more time for a neighbouring patch to also obtain a number of infected people that can start an epidemic.

A stricter quarantine (decreasing the minimum number of infected) or an even better medicine (increasing recovery rate) can amplify these effects. In table 4.1 the maximum number of infectious is shown in certain patches for the different possible measures. Which patches are studied is shown in figure 4.8. These patches are chosen, because of their different locations and distances with respect to the initial infection patch.

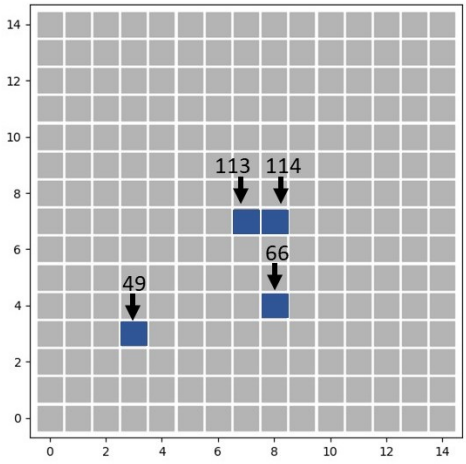

Figure 4.8: Patches studied in table 4.1

	Patch	113	Patch	114	Patch	66	Patch	49
	T_{max}	I_{max}	T_{max}	I_{max}	T_{max}	I_{max}	T_{max}	I_{max}
No measures	10.5	265	20.5	258	44.3	258	66.0	258
Medicine $\gamma = 1/2$	10.5	265	20.5	258	45.9	150	72.0	150
Medicine $\gamma = 1$	10.5	265	20.5	258	55.3	37	100.0	31
Quarantine $I_p > 10$	10.5	266	27.9	262	50.8	262	72.3	262
Quarantine $I_p > 5$	10.5	266	59.2	257	83.3	262	100.0	93
Both $I_p > 10$, $\gamma = 1/2$	10.5	266	27.9	262	53.7	153.34	79.5	153.34

Table 4.1: Maximum number of infections and the corresponding time instance for different patches (112, 113, 66 and 49) for different measures taken.

Table 4.1 shows that the different measures not necessarily influence the patch where the first epidemic occurs. The different measures affect mostly the speed and intensity of the further spread. For the patches neighbouring the initial patch, like patch 13, the medicine does not influence the number of infections and the corresponding time this peak occurs. Since the medicine was only developed after 30 days, it can only influence patches that get infected after this moment. We do see that the quarantine influences the speed of spread to this patch. It appears that for the quarantine the smaller the minimum number of infections for quarantine is chosen, the slower the disease spreads between the patches. The number of infections is not lower (even a little higher), but the total number of people that is sick at any given time is. If for example, an area has to deal with low treatment supplies, quarantine can make sure that the number of infections at one time is lower and therefore no shortages of supplies occur.

In table 4.1 it can be seen that after the developing period the medicine has a big influence on the number of infections and also on the speed of spread. The table shows that by decreasing the infection duration from 3 to 2 days the number of maximum infections for patches that can use this medicine decreases from 258 to 150. For an even better medicine that decreases the infection period to 1 day the maximum number of infections is even lower. Furthermore it can be noted that the spread between the patches becomes slower.

The best solution, according to table 4.1 is a combination of the two measures. By slowing down further spread of the disease using quarantine, less patches have been infected by the time a medicine is developed. More people therefore have access to the medicine when they become infected.

4.3 One reservoir

So far it was assumed that each patch has its own water supply. This model can represent for example a group of villages where each has its own water well. Another possibility of course is that multiple villages share the same water supply, therefore we will now consider a shared water reservoir. Equations 4.2-4.4 still hold, but equation 4.5 now has to be written as:

$$\frac{dB}{dt} = \sum_{p=1}^{n} \epsilon_p I_p + (g_b - l_b)B \tag{4.6}$$

where ϵ_p is again the influence of a single infected person on the bacterial concentration in the water in each patch. This parameter can vary for each patch (village), since different villages might have different accessibility to the water. This one-reservoir model has also been implemented. In figure 4.9 the number of infected is shown for each of the patches at different time instances.

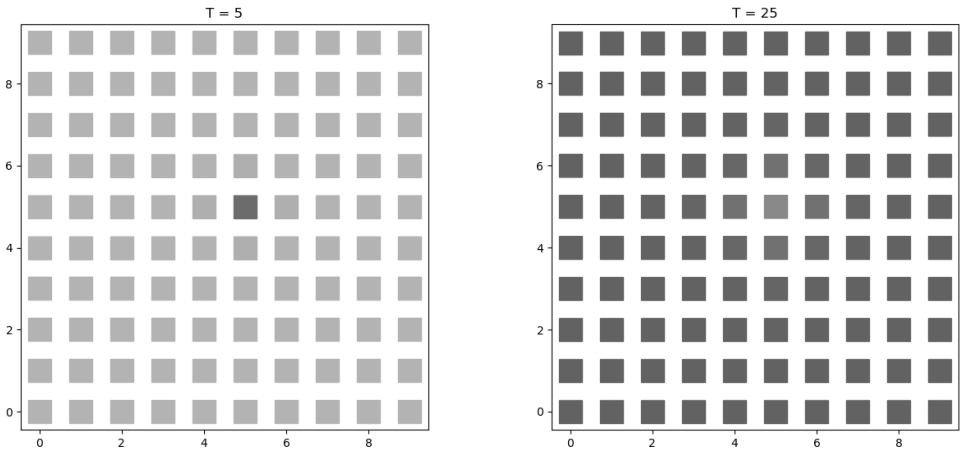

(a) 5 days

(b) 10 days

Figure 4.9: Number of infected people at multiple time instances for the SIRB patches model for $m_{pq} = 0.01$, $\epsilon_p = 0.01$, $\beta_e = \frac{1}{40}$

Due to infections in the initial patch the bacterial concentration in the water increases. Since the water reservoir is shared between the entire domain, in all patches people will get infected due to the cholera bacteria inside the water. This is exactly what we see in the second picture. The number of infections due to infected water is much larger then the number of infections due to human interaction. Therefore all patches will start their epidemic almost at the same time, when we include this shared reservoir in our model. By decreasing the environmental impact β_e the outward spreading pattern we saw earlier comes back.

4.4 River

The patches model is a very flexible model. Since the parameters can be taken patch depended, the spatial model is a simple method to study the influence of different circumstances in each of the patches. An environmental impact that can be researched is for example a river going through some of the patches. People living near the river can get infected faster than people who do not have the same contact with the water source. We will consider such a river going through our domain. Two assumptions are made. Firstly, infections due to the environment (the cholera bacterial concentration) only happen in patches where the river runs through. The infections that arise in non-river patches are exclusively caused by human interaction and migration. Secondly, the spreading of the bacteria through water is simulated using migration. So for the river patches an extra term is added to equation 4.5:

$$\frac{dB_p}{dt} = \epsilon_p I_p + (g_{bp} - l_{bp})B_p + \sum_{q=1}^{n} (bm_{pq}B_q - bm_{qp}B_p) \tag{4.7}$$

where bm_{pq} is the migration number of the bacteria from patch q to p. This bacterial migration number can be used to simulate the flow direction of the river water. The model has been implemented for an upward stream. For the upward migration the parameter was chosen as $bm = 0.1$ and for downward migration as $bm = 0.05$. For the people living in the river patches the rate of exposure to the water is $\beta_e = \frac{1}{4}$. For the non-river patches the value was set to zero. In figure 4.10 the number of infected is presented.

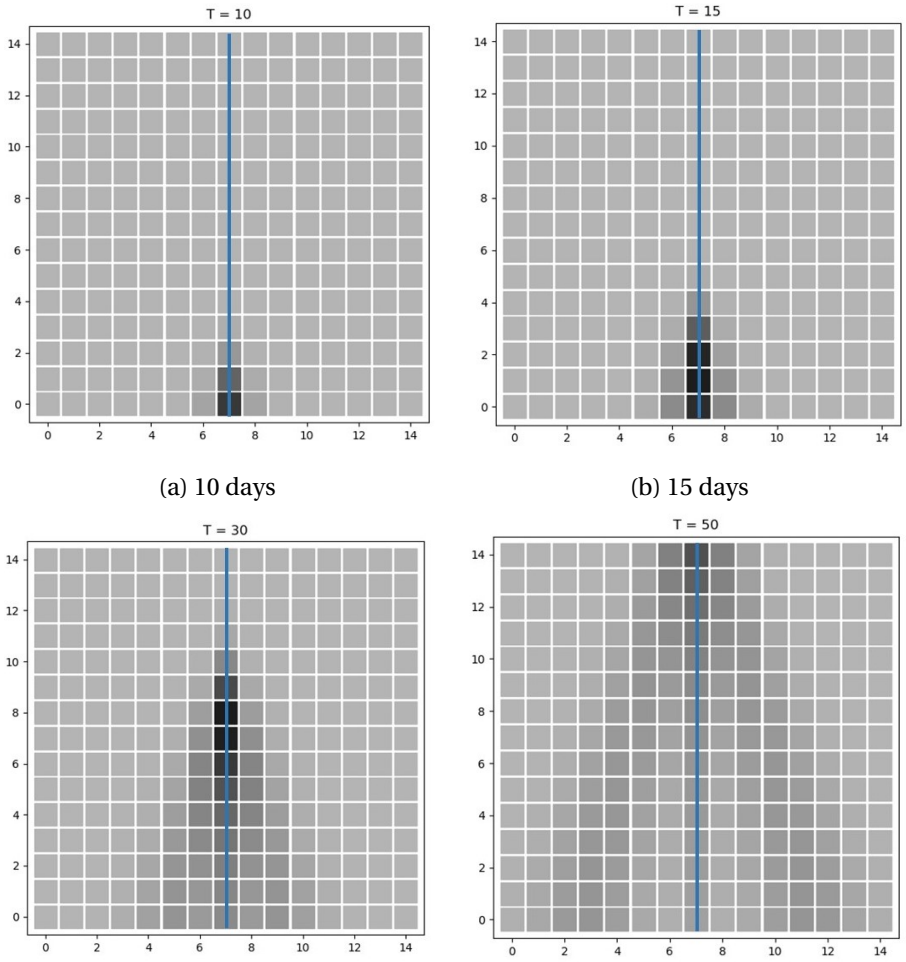

(a) 10 days

(b) 15 days

(c) 30 days

(d) 50 days

Figure 4.10: Number of infected people at multiple time instances for the SIRB patches model for $m_{pq} = 0.03$ (matrix structure $15x15$). Initial infection at beginning (bottom) of the river

The figure above reveals that most infections happen at river patches. This makes sense since the only environmental infections occur there. In figure 4.10a the initial infection is shown at the bottom of the river. It can be seen that the bacteria spreads itself through the water and creates new infections inside these patches. From the river patches the infections spread to the outward patches by means of human migration. There the number of infections is a lot less, since they are not in contact with infected water. In figure 4.11 on the next page the bacterial concentration of different river patches is shown for the model described above.

In figure 4.11 it can be seen that indeed the *V. cholerae* spreads upwards the river. The peak in bacterial concentration in the initial patch (7) is lower than in the patches further up the river (97 and 172). This might be explained by the fact that these patches are positioned further up the stream and get diffusion from both patches upward and downward the river. During the epidemic of the initial infection patch it is the only patch with a high amount of *V. cholerae* in their part of the river. They do not receive as much bacteria from other river patches.

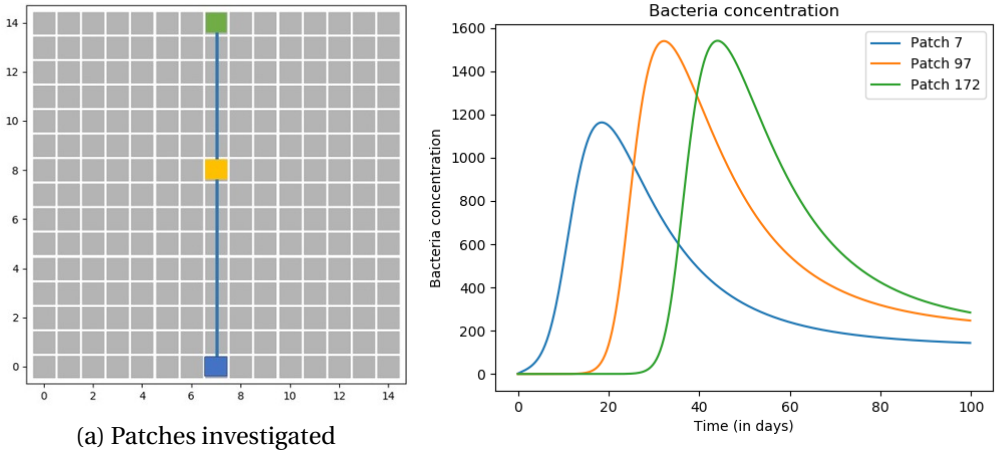

(a) Patches investigated

(b) Bacterial concentration over a period of 100 days

Figure 4.11: Bacterial concentration of different selected patches over a period of 100 days for the SIRB patches model for $m_{pq} = 0.03$. Initial infection at beginning (bottom) of the river

As explained earlier the bacterial migration number bm can simulate the flow direction of the water. To show that effect more clearly, in figure 4.12 the number of infected is shown at three time instances. The upward migration was chosen as $bm = 0.1$ and the downward migration as $bm = 0.025$. Figure 4.12b illustrates that after 25 days the disease has spread faster upward than downward. This coincides with what would be expected for a river with upward stream.

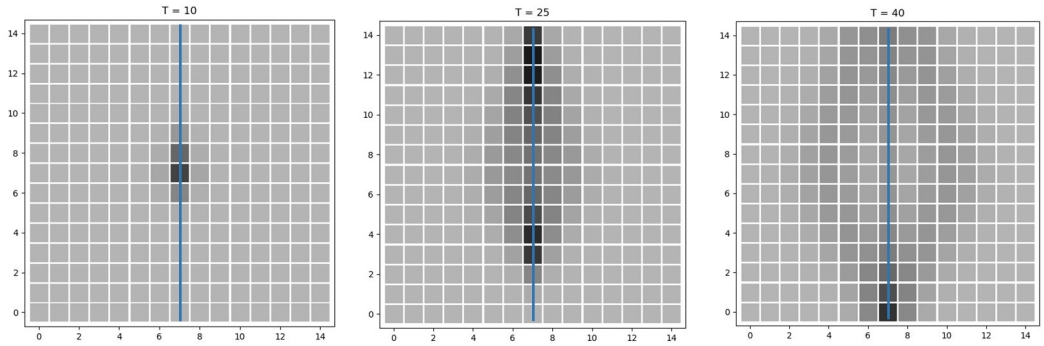

(a) 10 days

(b) 25 days

(c) 40 days

Figure 4.12: Number of infected people at multiple time instances for the SIRB patches model for $m_{pq} = 0.03$ (matrix structure $15x15$). Initial infection at the middle of the river

4.5 Discussion

The examples in this section already show the flexibility of the patches model. Since the parameters can be taken patch dependent and the migration between the patches can be customised, the model is very adaptable. In this section it was shown that different measures can be tested and different environmental situations can be simulated. This makes the patches model widely applicable to many different circumstances.

However the patches model requires a situation where the population can be divided into different patches. Sometimes it can be desirable to consider a more continuous spread inside a population. This way general spreading patterns inside a population can be studied. Adding diffusion to the original system could have this effect.

5 SPATIAL SIRB DIFFUSION MODEL

In this section a spatial diffusion model will be implemented and studied. The model will be applied to two different initial situations: one point spread and random spread.

5.1 DERIVATION DIFFUSION MODEL

The SIRB model of Coveço et al. [6] was further extended by Mawuena Afi and Anas [10] by adding a spatial aspect. It was again assumed that the population size is fixed. By making this assumption the third equation can be left out. The recovered group of the population is then $N-S-I$. Since the distribution of individuals can be considered as random, Fick's law holds and therefore we can add diffusion terms to the differential equations (2.7-2.10) [19]. The following spatial system is obtained:

$$\frac{dS}{dt} = -\frac{\beta_h IS}{N} - \mu S + \Gamma N - \beta_e \lambda(B) S + D_1 \nabla^2 S \tag{5.1}$$

$$\frac{dI}{dt} = \frac{\beta_h IS}{N} - \gamma I - \mu I + \beta_e \lambda(B) S + D_2 \nabla^2 I \tag{5.2}$$

$$\frac{dB}{dt} = \epsilon I + (g_b - l_b) B + D_3 \nabla^2 B \tag{5.3}$$

where ∇^2 is the two dimensional Laplacian operator and D_1, D_2 and D_3 are the diffusion coefficients. Furthermore we will consider Neumann boundary conditions at the boundary of our domain $\partial\Omega$:

$$\frac{\partial S}{\partial \mathbf{n}} = \frac{\partial I}{\partial \mathbf{n}} = \frac{\partial B}{\partial \mathbf{n}} = 0 \tag{5.4}$$

A two dimensional finite difference scheme has been implemented to simulate the solution of this model. Applying a double uniform grid with spatial step dx gives the following Euler Forward time stepping scheme:

$$S_{i,j}^{t+1} = S_{i,j}^t + dt\left(\frac{dS_{i,j}^t}{dt} + D_1 \nabla^2 S_{i,j}^t\right) \tag{5.5}$$

$$I_{i,j}^{t+1} = I_{ij}^t + dt\left(\frac{dI_{i,j}^t}{dt} + D_2 \nabla^2 I_{i,j}^t\right) \tag{5.6}$$

$$B_{i,j}^{t+1} = B_{i,j}^t + dt\left(\frac{dB_{i,j}^t}{dt} + D_3 \nabla^2 B_{i,j}^t\right) \tag{5.7}$$

where i and j are the nodes in the x and y direction and where $\frac{dS_{i,j}^t}{dt}$, $\frac{dI_{i,j}^t}{dt}$ and $\frac{dB_{i,j}^t}{dt}$ are the same equations as 2.7, 2.8 and 2.10 at each of the nodes. The Laplacian is discretized as follows:

$$\nabla^2 u_{i,j} = \frac{-4u_{i,j} + u_{i+1,j} + u_{i-1,j} + u_{i,j+1} + u_{i,j-1}}{dx^2} \tag{5.8}$$

We will consider a two dimensional area where $x, y \in [0, 20]$. The above model was discretized through $x \to (x_0, x_1, x_2, ..., x_N)$ and $y \to (y_0, y_1, y_2, ..., y_N)$ where $N = 200$, so $dx = 0.1$. The time step was chosen as $dt = 0.005$. An Euler forward time stepping scheme has been used to approximate the solution. [20] [21] The derivation of the specific scheme can be found in appendix D.

5.2 ONE POINT SPREAD

On the next page two figures are shown that illustrate the spread of infected people from the centre. In figure 5.1 the spread is presented for diffusion constants $D_1 = D_2 = D_3 = 0.01$. It can be seen that the outward spread of the disease is similar to that of the spatial patches model.

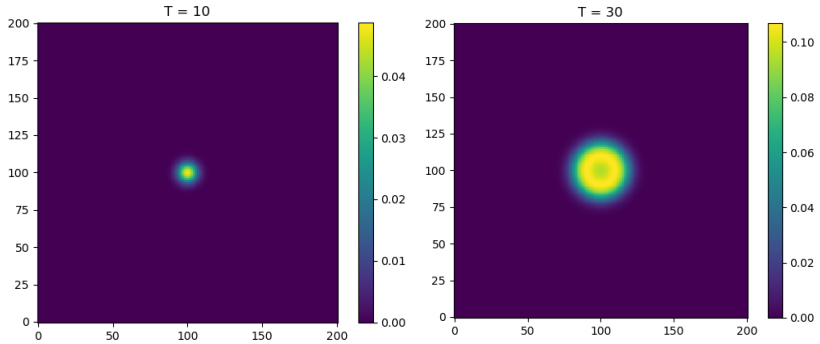

(a) 10 days (b) 30 days

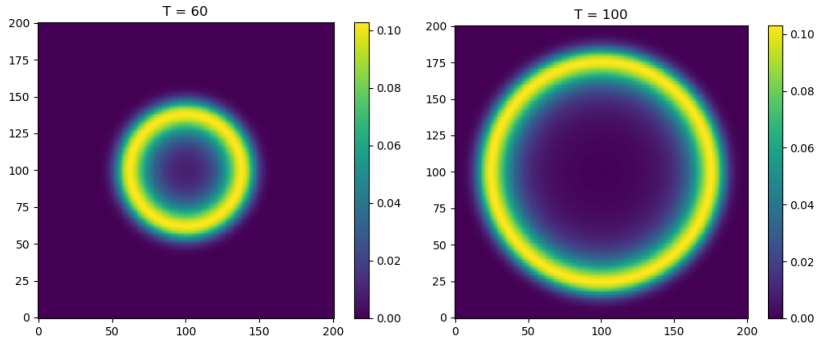

(c) 60 days (d) 100 days

Figure 5.1: Portion of infected people at multiple time instances for the SIRB model using diffusion for $D_1, D_2, D_3 = 0.01$

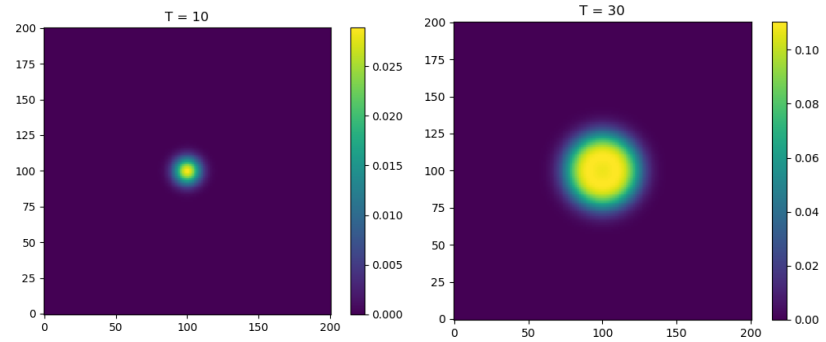

(a) 10 days (b) 30 days

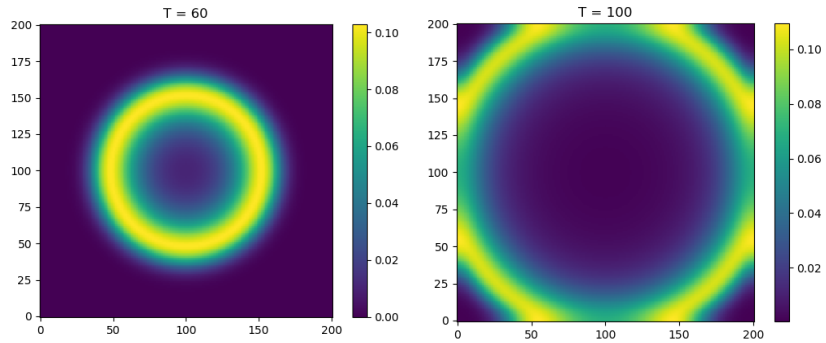

(c) 60 days (d) 100 days

Figure 5.2: Portion of infected people at multiple time instances for the SIRB model using diffusion for $D_1, D_2, D_3 = 0.02$

In figure 5.2 the spread is shown for two times larger diffusion constants, so $D_1 = D_2 = D_3 = 0.02$. It can be observed that for larger diffusion constants cholera spreads faster. A comparison can be made with increasing the migration constant inside the spatial patches model, described in the previous section.

Next two situations are considered: no diffusion of bacteria throughout the domain ($D_3 = 0$) and bacteria diffusion throughout the domain ($D_3 = 0.04$). When no diffusion of bacteria is taken into account, the growth of the bacterial concentration in a certain node is only possible if the node gets infected due to diffusion of infected individuals. In figure 5.3 the spread of the two different diffusion rates is presented at $T = 60$ days. It can be seen that the spreading of the disease goes faster when the diffusion term is added. This is in agreement with what one would expect. By applying diffusion to the bacterial concentration of infected nodes, the water of other nodes gets infected faster (not only due to infected individuals). When we translate this to the real world we can relate the fact that there is no bacterial diffusion to everyone having their own clean water supply. The cholera bacteria cannot spread between the water in the different households, but it is possible to get infected by water that is contaminated by someone else inside the household.

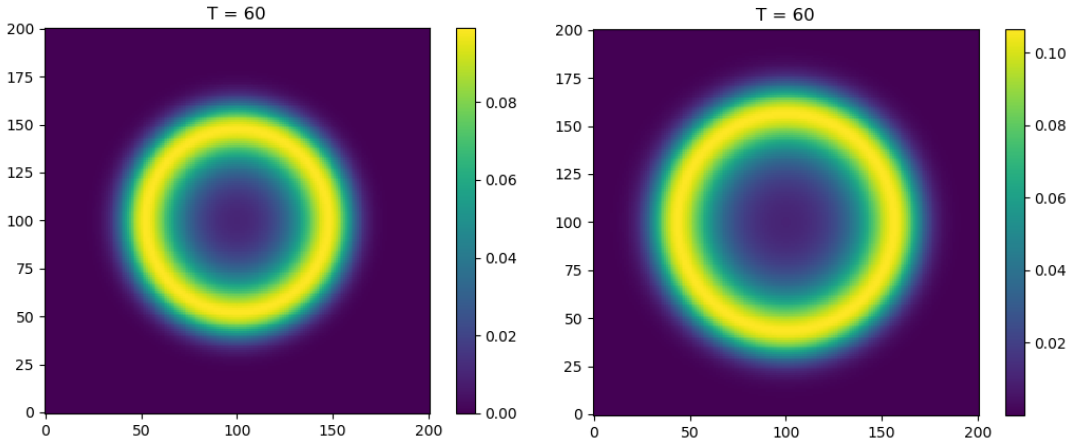

(a) 60 days ($D_3 = 0$)

(b) 60 days ($D_3 = 0.04$)

Figure 5.3: Portion of infected people at $T = 60$ the SIRB model without diffusion of bacterial concentration ($D_3 = 0$) and with diffusion ($D_3 = 0.04$)

Although the diffusion model is not as flexible as the patches model, it is possible to look at other initial situations. Instead of starting the infection wave inside one node, the infection could start for example in two different nodes, such as is shown in figure 5.4.

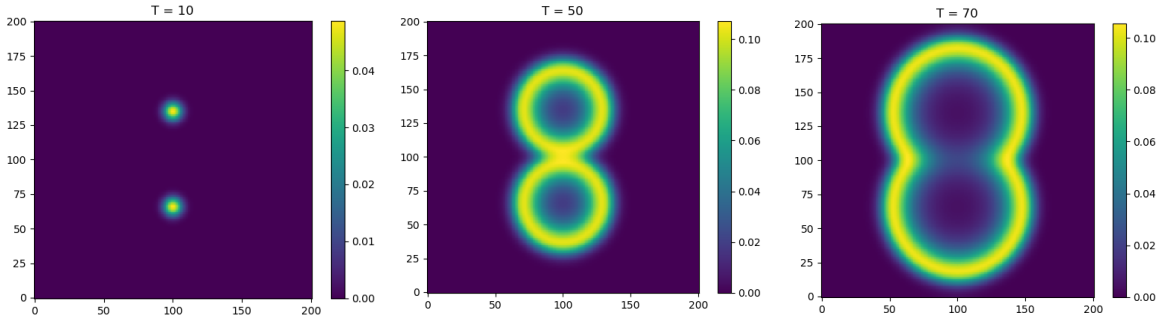

(a) 10 days

(b) 50 days

(c) 70 days

Figure 5.4: Portion of infected people at different time instances using the SIRB model with $D_1 = D_2 = D_3 = 0.02$ and the initial infection starting at two nodes

One might expect that the two different infection spreads (waves) cause an interference pattern. However in figure 5.4 it can be seen that no such pattern forms. Since the number of susceptibles is very low in the regions where the disease already occurred a second infection wave is not possible, until some time has passed for the group of susceptibles to grow due to birth of newborns. So therefore 5.4 illustrates that the two infection waves merge and cause further spread of cholera.

5.3 Random spread

Another possible initial situation is a random pattern as shown in figure 5.5a. The initial number of infected people I_0 inside each node was randomly selected between 0 and 0.001 and the total number of people in each node has been taken 1. It can be seen in figures 5.5b-5.5d that due to diffusion the pattern becomes smoother over time.

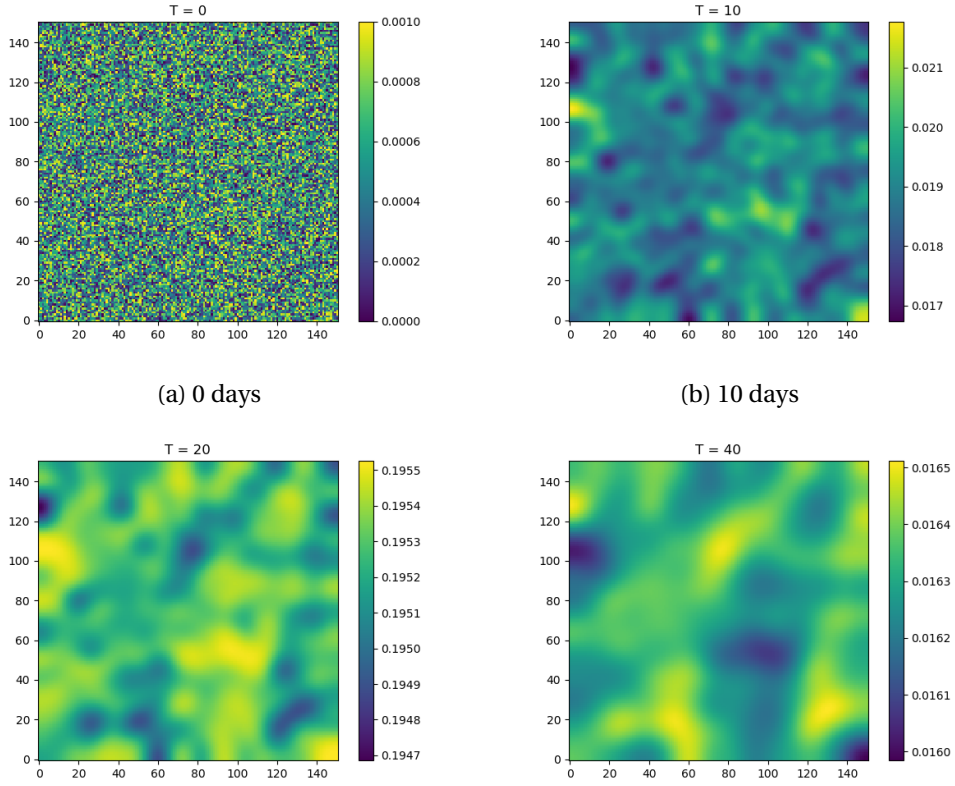

(a) 0 days

(b) 10 days

(c) 20 days

(d) 40 days

Figure 5.5: Portion of infected people at multiple time instances for the SIRB model using random initial conditions and $D_1 = D_2 = D_3 = 0.01$

By increasing the diffusion constants the number of infected is more spread and the patterns become more smooth. This is shown in figure 5.6, where the diffusion constants were taken as $D_1 = D_2 = D_3 = 0.02$. The exact same random situation as in figure 5.5 was used, but we see that at the same instances the pattern looks more smooth for the model with higher diffusion. If we consider the maximum values of infected for both the low and high diffusion, we see that at each time instances these are nearly the same. In this case the diffusion constants do not seem to influence the number of infected, but do influence how they are spread over the domain. To confirm this finding, for another random initial situation the average number of infected was calculated at different time instances and for different diffusion constants. In table 5.1 the results are shown.

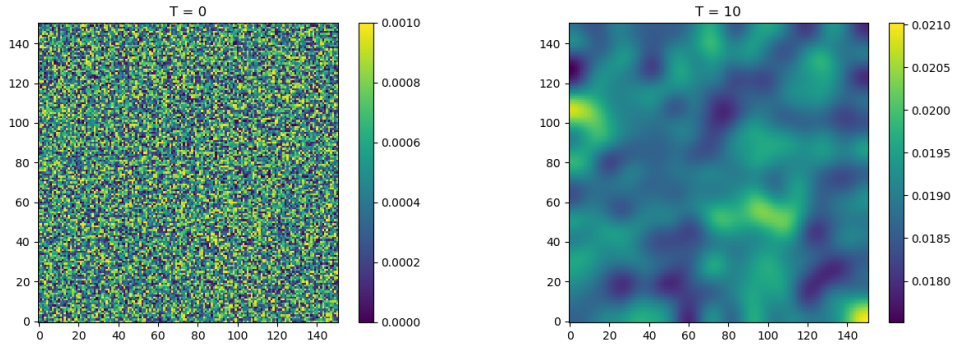

(a) 0 days

(b) 10 days

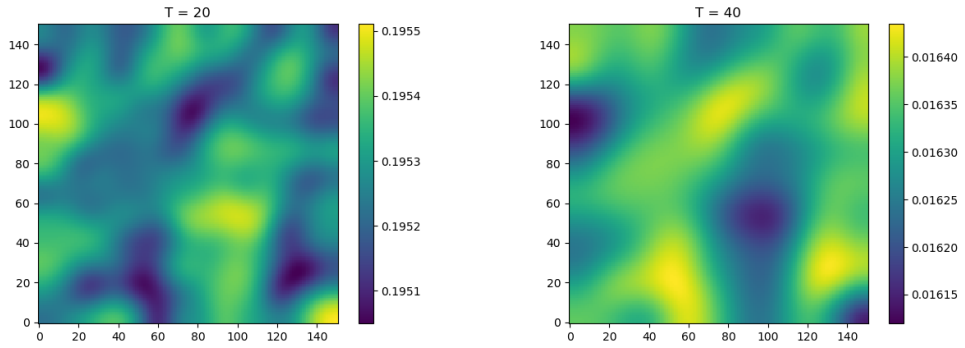

(c) 20 days

(d) 40 days

Figure 5.6: Portion of infected people at multiple time instances for the SIRB model using random initial conditions and $D_1 = D_2 = D_3 = 0.02$

D_1, D_2, D_3	10 days Average	Maximum	Minimum	20 days Average	Maximum	Minimum
0.01	0.01901	0.02147	0.01671	0.19527	0.19552	0.19467
0.02	0.01902	0.02082	0.01749	0.19529	0.19551	0.19497
0.06	0.01902	0.01995	0.01830	0.19530	0.19543	0.19513
0.10	0.01902	0.01967	0.01967	0.19530	0.19540	0.19515

Table 5.1: Average, maximum and minimum number of infected for different diffusion constants $D_1, D_2, D_3 = [0.01, 0.02, 0.06, 0.10]$ at different time instances 10 and 20 days.

In table 5.1 it can be seen that the average number of infected is (almost) the same for all values of the diffusion constants. The differences however can be found in the minimums and maximums. For low values of the diffusion constant there is more variety between the minimum, maximum and average. For large values of the diffusion constant the pattern is very smooth and therefore the minimum, maximum and average will be relatively close together. However the table illustrates that at a later time instance (in this case 20 days) the difference between the maximums of the diffusion constants decreases. This can be explained, since at this point all models are more evenly spread due to diffusion and the differences become smaller. To show the influence of the diffusion constants even better the model has also been plotted in 3D. This is presented in figure 5.7.

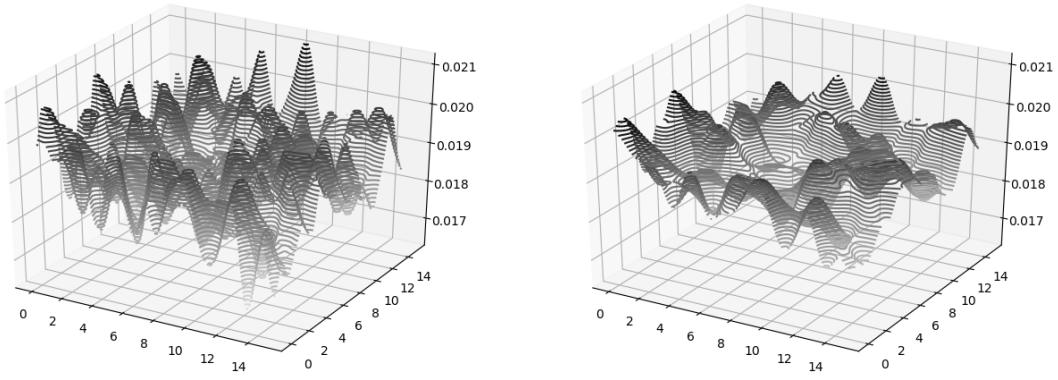

(a) $D_1, D_2, D_3 = 0.01$ (b) $D_1, D_2, D_3 = 0.02$

Figure 5.7: Portion of infected people at 10 days for the SIRB model using random initial conditions and two different values for the diffusion constants

In the 3D figure above the influence of the diffusion coefficient is very clear. The figure supports the findings from table 5.1. As we already saw in figures 5.5 and 5.6 the pattern for a higher value of diffusion is smoother than for a lower value. The 3D image illustrates clearly that the peaks in infections are less high.

5.4 Discussion

Although the diffusion model is less flexible than the patches model it can still be used to study spreading patterns of airborne diseases. In this section we saw that it can be applied to different initial situations. The diffusion constants D_1, D_2 and D_3 turned out to influence the speed of spatial spread and the smoothness of the patterns arising.

Certain epidemic patterns that are studied are so called Turing patterns. [11] [22] [23] In 1952 Turing [24] suggested that passive diffusion could interact with reaction in such a way that diffusion could destabilise the symmetric solutions of the reaction-diffusion model. When this happens Turing patterns occur. Turing patterns can be found in nature, chemistry and also in epidemic models if the parameters are properly chosen. The epidemic diffusion models can then give rise to Turing stationary patterns as a result of diffusion. [22]

In this section we already saw some patterns arising from the diffusion model, but a study into Turing stability and patterns arising from diffusion driven instability, would give better insight in under which circumstances these patterns could occur. Very little research has yet been done into Turing patterns for epidemic models concerning indirect infectious diseases, like cholera.

6 CONCLUSION

The reproduction number R_0 turns out to be one of the most important indicators to see if an infectious disease will cause a large epidemic. In chapter 3 it has been shown that when $R_0 < 1$ the solution will go to the disease free equilibrium. This DFE only turns out to be stable for $R_0 < 1$. When R_0>1 there are two equilibrium solutions: the disease free equilibrium and the endemic equilibrium. Since the DFE is unstable for these values of the reproduction number the solution will go to the EE unless the initial state is the DFE.

Furthermore two spatial extensions to the SIRB model have been considered. The spatial patches model turned out to be a very flexible model. Two different measures against the infectious disease cholera, quarantine and medicine, were studied for the different patches. Since developing a medicine takes time there is no short term influence of this measure on the number of infected. Long term a medicine can drastically decrease the number of infected. Quarantine, on the other hand, does not influence the number of infected inside each of the patches, but does slow the spread of the disease between the patches. This can be useful when there is for example a chance on shortages of supplies. A combination of both measures would give the most optimal situation; the spread of cholera is slowed by quarantine, until a medicine is produced.

Using the patches model, it is not only possible to study the influence of certain measures against cholera, but it is also quite easy to incorporate other environmental circumstances, such as a river. The best feature of the patches model is likely the flexibility. Different parameters can be taken in each of the patches and the migration between the patches can also be customised. The patches model can therefore be used to study a wide range of circumstances.

The diffusion model might be a little less flexible, but does give general information about pattern formation. The results for disease spread originating in one point is similar to that of the patches model. By increasing the diffusion coefficients the disease will spread faster to the boundary of the domain, but the number of infections will be the same as for a low diffusion number. When considering an initial situation with random infection spread it can be concluded that the diffusion coefficients influence the smoothness of the solutions. For the random initial situation a pattern of peaks and holes appears. For a larger diffusion number these peaks are less high and more smooth.

Further research into these spatial cholera models would definitely be worthwhile. A cholera infection can be deadly if not treated fast (within a few hours).[3] The treatment consists simply of hydration. The mortality of the disease was not currently taken into account. It could be interesting to study the influence of this mortality on the total number of infections. Furthermore, the flexibility of the diffusion model could be challenged by for example trying to implement different measures against cholera inside the model. Also environmental impacts could possibly be implemented. More research into pattern formation for the diffusion model of cholera would be recommended. A study into Turing instability for spatial cholera models will provide more information about certain patterns that can arise from these models.

Lastly it would be interesting to verify the spatial models with existing data of cholera epidemics. Especially the patches model can be used to simulate the spread of cholera between different villages in a certain region. The primary reason for mathematical modelling of infectious diseases is to get a better understanding of how the disease will develop inside a population and study possible measures that can minimise this spread. By linking the mathematical models for cholera to real data we get closer to the goal of understanding the disease spread in certain regions.

REFERENCES

[1] RIVM. *Cholera*. 2018. URL: https://www.rivm.nl/cholera.

[2] Centers for Disease Control and Prevention. *Cholera-Vibrio cholerea infection*. 2018. URL: https://www.cdc.gov/cholera/general/index.html.

[3] World Health Organisation. *Cholera*. 2019. URL: https://www.who.int/news-room/fact-sheets/detail/cholera#:~:text=History,and%20the%20Americas%20in%201991..

[4] Herbert W Hethcote. "The mathematics of infectious diseases". In: *SIAM review* 42.4 (2000), pp. 599–653.

[5] Joseph H Tien and David JD Earn. "Multiple transmission pathways and disease dynamics in a waterborne pathogen model". In: *Bulletin of mathematical biology* 72.6 (2010), pp. 1506–1533.

[6] Cláudia Torres Codeço. "Endemic and epidemic dynamics of cholera: the role of the aquatic reservoir". In: *BMC Infectious diseases* 1.1 (2001), p. 1.

[7] Zindoga Mukandavire et al. "Estimating the reproductive numbers for the 2008–2009 cholera outbreaks in Zimbabwe". In: *Proceedings of the National Academy of Sciences* 108.21 (2011), pp. 8767–8772.

[8] Jianjun Paul Tian and Jin Wang. "Global stability for cholera epidemic models". In: *Mathematical biosciences* 232.1 (2011), pp. 31–41.

[9] Gui-Quan Sun et al. "Transmission dynamics of cholera: Mathematical modeling and control strategies". In: *Communications in Nonlinear Science and Numerical Simulation* 45 (2017), pp. 235–244.

[10] Havor Phebe Mawuena Afi. "Dynamics of disease models with self-diffusion: A study of cholera". In: (2015).

[11] Gui-Quan Sun. "Pattern formation of an epidemic model with diffusion". In: *Nonlinear Dynamics* 69.3 (2012), pp. 1097–1104.

[12] William Ogilvy Kermack and Anderson G McKendrick. "A contribution to the mathematical theory of epidemics". In: *Proceedings of the royal society of london. Series A, Containing papers of a mathematical and physical character* 115.772 (1927), pp. 700–721.

[13] Jane M Heffernan, Robert J Smith, and Lindi M Wahl. "Perspectives on the basic reproductive ratio". In: *Journal of the Royal Society Interface* 2.4 (2005), pp. 281–293.

[14] Pauline van den Driessche. "Reproduction numbers of infectious disease models". In: *Infectious Disease Modelling* 2.3 (2017), pp. 288–303.

[15] G.J. Olsder et al. *Mathematical Systems Theory*. 4th ed. VSSD, 2011.

[16] Wendi Wang and G Mulone. "Threshold of disease transmission in a patch environment". In: *Journal of Mathematical Analysis and Applications* 285.1 (2003), pp. 321–335.

[17] Julien Arino, Richard Jordan, and P Van den Driessche. "Quarantine in a multi-species epidemic model with spatial dynamics". In: *Mathematical biosciences* 206.1 (2007), pp. 46–60.

[18] Marisa C Eisenberg et al. "A cholera model in a patchy environment with water and human movement". In: *Mathematical Biosciences* 246.1 (2013), pp. 105–112.

[19] Li Li. "Patch invasion in a spatial epidemic model". In: *Applied Mathematics and Computation* 258 (2015), pp. 342–349.

[20] C. Vuik et al. *Numerical Methods for Ordinary Differential Equation*. 2nd ed. Delft: Delft Academic Press/VSSD, 2018.

[21] J. van Kan et al. *Numerical Methods for Partial Differential Methods*. Delft Academic Press/VSSD, 2019.

[22] Weiming Wang et al. “Complex dynamics of a reaction–diffusion epidemic model”. In: *Nonlinear Analysis: Real World Applications* 13.5 (2012), pp. 2240–2258.

[23] Weiming Wang et al. “Turing patterns in a diffusive epidemic model with saturated infection force”. In: *Journal of the Franklin Institute* 355.15 (2018), pp. 7226–7245.

[24] Alan Mathison Turing. “The chemical basis of morphogenesis”. In: *Bulletin of mathematical biology* 52.1-2 ((1952)1990), pp. 153–197.

A FINITE DIFFERENCE MATRIX

The Laplacian operators in equations 5.1-5.3 have been discretized as follows:

$$\nabla^2 u_{i,j} = \frac{-4u_{i,j} + u_{i+1,j} + u_{i-1,j} + u_{i,j+1} + u_{i,j-1}}{dx^2}$$

Discretizing through $x \rightarrow (x_0, x_1, x_2, ..., x_N)$ and $y \rightarrow (y_0, y_1, y_2, ..., y_N)$ and applying Neumann boundary conditions at the boundary of the domain the following scheme can be obtained:

$$S_{t+1} = S_t + dt\frac{dS_t}{dt} + dtD_1 AS_t \tag{A.1}$$

$$I_{t+1} = I_t + dt\frac{dI_t}{dt} + dtD_2 AI_t \tag{A.2}$$

$$B_{t+1} = B_t + dt\frac{dB_t}{dt} + dtD_3 AB_t \tag{A.3}$$

where S_t. I_t and B_t are in lexicographic order and A can be determined using the boundary conditions and the discretization of the Laplacian:

$$\nabla^2 X_{i,j} = \frac{-4X_{i,j} + X_{i+1,j} + X_{i-1,j} + X_{i,j+1} + X_{i,j-1}}{h^2}$$

applying Neumann boundary conditions:

$$\nabla^2 X_{0,0} = \frac{-4X_{0,0} + 2X_{0,1} + 2X_{1,0}}{h^2}$$
$$\nabla^2 X_{1,0} = \frac{-4X_{1,0} + X_{0,0} + X_{2,0} + 2X_{1,1}}{h^2}$$
$$\nabla^2 X_{0,N_y} = \frac{-4X_{0,N_y} + 2X_{1,N_y} + 2X_{0,N_y-1}}{h^2}$$
$$\nabla^2 X_{1,N_y} = \frac{-4X_{1,N_y} + X_{0,N_y} + X_{2,N_y} + 2X_{1,N_y}}{h^2}$$
$$\nabla^2 X_{2,0} = \frac{-4X_{2,0} + X_{3,0} + X_{1,0} + 2X_{2,1}}{h^2}$$
$$\nabla^2 X_{N_x,0} = \frac{-4X_{N_x,0} + 2X_{N_x-1,0} + 2X_{N_x,1}}{h^2}$$
$$\nabla^2 X_{N_x,2} = \frac{-4X_{N_x,2} + 2X_{N_x-1,2} + X_{N_x,1} + X_{N_x,3}}{h^2}$$

So the following matrix is obtained for A:

$$A = \frac{1}{h^2}\begin{bmatrix}
-4 & 2 & 0 & & & 2 & & & & & & \\
1 & -4 & 1 & 0 & & & 2 & & & & & \\
0 & 1 & -4 & 1 & 0 & & & 2 & & & & \\
\vdots & & \ddots & \ddots & \ddots & \ddots & & & \ddots & & & \\
0 & & & 2 & -4 & 0 & & & & 2 & & \\
1 & & & & 0 & -4 & 2 & & & & 1 & \\
0 & 1 & & & & 1 & -4 & 1 & & & & 1 \\
 & & \ddots & & & & \ddots & \ddots & \ddots & & & \ddots \\
 & & & 2 & & & & 0 & -4 & 2 & & \\
 & & & 0 & 2 & & & & 0 & 1 & -4 & 1 \\
 & & & & 0 & 2 & & & & & 2 & -4
\end{bmatrix}$$

B CODE SIRB MODEL

The code below belongs to the non-spatial SIRB model discussed in section 2.2

```
import matplotlib.pyplot as plt
import numpy as np

#Initial values
S = 1000
I = 10
R = 0
B = 0
N = S+I+R

#Timestep and endtime
dt = 0.01
T = 100

#Transmission constants
B_h = 1/2           #Human-human
B_e = 1/4           #Environment-human
g = 1/3             #Recovery rate
m = 0.001           #Mortality
k = 0.001           #Birth rate
a = 0#5             #Disease induced mortality
eps =1              #Infected people-water
nb = 0.1            #Cholera loss in water
mb = 0              #Cholera growth in water

#Functions for calculating dt
def dtS(S,I,R,B,N):
    return - B_h*I*S/N-m*S+k*N-B_e*B*S

def dtI(S,I,R,B,N):
    return B_h*I*S/N-(g+m+a)*I+B_e*B*S

def dtR(S,I,R,B,N):
    return g*I-m*R

def dtB(S,I,R,B,N):
    return eps*I-(nb-mb)*B

#Using Euler Forward to calculate epidemic
def Epidemic (S,I,R,B,N,dt,T):
    S_list,I_list,R_list,B_list,N_list =[],[],[],[],[]
    for i in range (int(T/dt)):
        #Make copies
        Sc,Ic,Rc,Bc = S,I,R,B
        #Caculate newvalues
        S = Sc + dt * dtS(Sc,Ic,Rc,Bc,N)
        I = Ic + dt * dtI(Sc,Ic,Rc,Bc,N)
        R = Rc + dt * dtR(Sc,Ic,Rc,Bc,N)
```

```
        B = Bc + dt * dtB(Sc,Ic,Rc,Bc,N)
        N = S+I+R
        S_list.append(S)
        I_list.append(I)
        R_list.append(R)
        B_list.append(B)
        N_list.append(N)
    return S_list,I_list,R_list,B_list,N_list
```

C Code Patches model

The code below belongs to the spatial patches model discussed in chapter 4. An Euler forward scheme has been used.

```
import matplotlib.pyplot as plt
from mpl_toolkits.mplot3d import Axes3D
import numpy as np

#Spatial patches model:

np_x = 15 #Patches in x direction
np_y = 15 #Patches in y direction

np_t = np_x*np_y #Total number of patches

#Initial values in each of the patches:
S = np.array([1000 for patch in range(np_t)],dtype=float)
I = np.array([0 for patch in range(np_t)],dtype=float)
R = np.array([0 for patch in range(np_t)],dtype=float)
B = np.array([0 for patch in range(np_t)],dtype=float)
#Start of disease:
I[112] = 10

N = S+I+R

#Parameters:
B_h = 1/2
B_e = 1/4
g = 1/3
mu = 0.001
k = 0.001
e = 1
g_b =0
l_b =0.1
c =1000

#Time
dt = 0.1
T = 100

#Create Migration
m = np.zeros((np_t,np_t))
mi = 0.001
for i in range(np_t):
    #Top left corner
    if i==0:
        m[i][i+np_x] = mi
        m[i][i+1] = mi
    #Top row
    elif i<(np_x-1):
        m[i][i+1]=mi
```

```
            m[i][i-1]=mi
            m[i][i+np_x]=mi
        #Top right corner
        elif i==np_x-1:
            m[i][i-1]=mi
            m[i][i+np_x]=mi
        #Bottom left corner
        elif i ==(np_x*np_y-np_x):
            m[i][i+1]=mi
            m[i][i-np_x]=mi
        #Bottom row
        elif i <(np_x*np_y-1) and i>(np_x*np_y-np_x):
            m[i][i+1]=mi
            m[i][i-1]=mi
            m[i][i-np_x]=mi
        #Bottom right corner
        elif i == (np_x*np_y-1):
            m[i][i-1]=mi
            m[i][i-np_x]=mi
        #Left row
        elif (i%np_x)==0:
            m[i][i+1]=mi
            m[i][i+np_x]=mi
            m[i][i-np_x]=mi
        #Right row
        elif ((i+1)%np_x)==0:
            m[i][i-1]=mi
            m[i][i+np_x]=mi
            m[i][i-np_x]=mi
        else:
            m[i][i-1]=mi
            m[i][i+1]=mi
            m[i][i+np_x]=mi
            m[i][i-np_x]=mi


def Epidemic (S,I,R,B,N,dt,T):
    S_matrix =np.zeros((np_t,int(T/dt)))
    I_matrix =np.zeros((np_t,int(T/dt)))
    R_matrix =np.zeros((np_t,int(T/dt)))
    B_matrix =np.zeros((np_t,int(T/dt)))
    N_matrix =np.zeros((np_t,int(T/dt)))
    for i in range (int(T/dt)):
        print(i)
        Sc,Ic,Rc,Bc,Nc = S,I,R,B,N
        for p in range(np_t):

            #Determine migration:
            Sm,Im,Rm = 0,0,0
            for q in range(np_t):
                mqp = m[q][p]
```

```
                mpq = m[p][q]
                Sm = Sm + Sc[q]*mqp - Sc[p]*mpq
                Im = Im + Ic[q]*mqp - Ic[p]*mpq
                Rm = Rm + Rc[q]*mqp - Rc[p]*mpq
            #Update new population
            Sp,Ip,Rp,Bp = Sc[p],Ic[p],Rc[p],Bc[p]
            S[p] = Sp + dt*(k*Nc[p]-mu*Sp-B_h*Sp*Ip/Nc[p]-B_e*Sp*(Bp/(Bp+c))+Sm)
            I[p] = Ip + dt*(B_h*Sp*Ip/Nc[p]-mu*Ip-g*Ip+B_e*Sp*(Bp/(Bp+c))+Im)
            R[p] = Rp + dt*(g*Ip-mu*Rp+Rm)
            N[p] = S[p]+I[p]+R[p]
            #And Bacteria
            B[p] = Bp + dt*(e*Ip+(g_b-l_b)*Bp)

            S_matrix[p][i] = S[p]
            I_matrix[p][i] = I[p]
            R_matrix[p][i] = R[p]
            B_matrix[p][i] = B[p]
            N_matrix[p][i] = N[p]
    return S_matrix,I_matrix,R_matrix,B_matrix,N_matrix

Sr,Ir,Rr,Br,Nr = Epidemic (S,I,R,B,N,dt,T)

time = np.array(range(int(T/dt)))*dt

#Plot infections in each patch
def plotEpidemic(Ir,T):
    timesegment = int(T/dt)
    for p in range(np_t):
        colores = Ir[p][timesegment-1]*-180.0/300.0+180
        plt.plot(p%np_x,int(p/np_x),marker = "s",markersize=20,
            color=(colores/255.0, colores/255.0, colores/255.0))
    plt.title(str(T))
    plt.show()
    return
```

For the study of the potential measures quarantine and a medicine the following Euler forward code has been used:

```
def Epidemic (S,I,R,B,N,dt,T):
    S_matrix =np.zeros((np_t,int(T/dt)))
    I_matrix =np.zeros((np_t,int(T/dt)))
    R_matrix =np.zeros((np_t,int(T/dt)))
    B_matrix =np.zeros((np_t,int(T/dt)))
    N_matrix =np.zeros((np_t,int(T/dt)))
    for i in range (int(T/dt)):
        #Condition for medicine
        if i>300:
            g = 1/2
        else:
            g=1/3
        Sc,Ic,Rc,Bc,Nc = np.copy(S),np.copy(I),np.copy(R),np.copy(B),np.copy(N)
        for p in range(np_t):
```

```
            #Determine migration:
            Sm,Im,Rm = 0,0,0
            for q in range(np_t):
                #Condition for quarantine
                if Ic[p]>10 or Ic[q]>10:
                    mqp = 0
                    mpq = 0
                else:
                    mqp = m[q][p]
                    mpq = m[p][q]
                Sm = Sm + Sc[q]*mqp - Sc[p]*mpq
                Im = Im + Ic[q]*mqp - Ic[p]*mpq
                Rm = Rm + Rc[q]*mqp - Rc[p]*mpq
            #Update new population
            Sp,Ip,Rp,Bp = Sc[p],Ic[p],Rc[p],Bc[p]
            S[p] = Sp + dt*(k*Nc[p]-mu*Sp-B_h*Sp*Ip/Nc[p]-B_e*Sp*(Bp/(Bp+c))+Sm)
            I[p] = Ip + dt*(B_h*Sp*Ip/Nc[p]-mu*Ip-g*Ip+B_e*Sp*(Bp/(Bp+c))+Im)
            R[p] = Rp + dt*(g*Ip-mu*Rp+Rm)
            N[p] = S[p]+I[p]+R[p]
            #And Bacteria
            B[p] = Bp + dt*(e*Ip+(g_b-l_b)*Bp)

            S_matrix[p][i] = S[p]
            I_matrix[p][i] = I[p]
            R_matrix[p][i] = R[p]
            B_matrix[p][i] = B[p]
            N_matrix[p][i] = N[p]
    return S_matrix,I_matrix,R_matrix,B_matrix,N_matrix
```

D Code Diffusion model

The code in this section belongs to chapter 5 where the diffusion SIRB model was discussed.

```
import numpy as np
import matplotlib.pyplot as plt
import scipy.sparse as sp
import scipy.sparse.linalg as la
import math
import random
from mpl_toolkits.mplot3d import Axes3D

xsize = 15
ysize = 15
dx = 0.1
Nx = int(xsize/dx)
Ny = int(ysize/dx)

#Grid point x and y
xgrid = [dx*i for i in range(0,Nx+1)]
ygrid = [dx*i for i in range(0,Ny+1)]

#Create the diagonals
def createA(Nx,Ny,dx,xsize,ysize,xgrid,ygrid):

    #Diagonal 1
    diagonal_1 =np.array([-4*dx**-2 for y in ygrid for x in xgrid ])
    #Diagonal 2
    diagonal_2 =np.array([1*dx**-2 for y in ygrid for x in xgrid])
    diagonal_2 = np.delete(diagonal_2,-1)
    pos_2 = [-2+(Nx+1)*(y+1) for y in range(Ny+1)]
    pos_0 = [-1+(Nx+1)*y for y in range(1,Ny+1)]
    for pos in pos_2:
        diagonal_2[int(pos)] = 2*dx**-2
    for pos in pos_0:
        diagonal_2[int(pos)] = 0
    #Diagonal 3
    diagonal_3 =np.array([1*dx**-2 for y in ygrid for x in xgrid])
    diagonal_3 = np.delete(diagonal_3,-1)
    pos_2 = [0+(Nx+1)*y for y in range(Ny+1)]
    pos_0 = [-1+(Nx+1)*y for y in range(1,Ny+1)]
    for pos in pos_2:
        diagonal_3[int(pos)] = 2*dx**-2
    for pos in pos_0:
        diagonal_3[int(pos)] = 0*dx**-2
    #Diagonal 4
    diagonal_4 =np.array([[1/dx**2 for x in xgrid] for y in ygrid[:-1]]).flatten()
    pos_2 = [(Nx+1)*(Ny)-x-1 for x in range(Nx+1)]
    for pos in pos_2:
        diagonal_4[int(pos)] =2*dx**-2
    #Diagonal 5
    diagonal_5 =np.array([[1/dx**2 for x in xgrid] for y in ygrid[1:]]).flatten()
```

```
    pos_2 = [x for x in range(Nx+1)]
    for pos in pos_2:
        diagonal_5[int(pos)] =2*dx**-2
    matrixsize = (Nx+1)*(Ny+1)

    L = sp.diags([diagonal_1,diagonal_2,diagonal_3,diagonal_4,diagonal_5],
        [0,-1,1,-(Nx+1),Nx+1],shape=(matrixsize,matrixsize),format="csc")

    return L

#Diffusion constants
D_1,D_2,D_3=0.01,0.01,0.01

#Time constants
dt = 0.01
endtime =10

#Other constants
B_h = 1./2.
B_e = 1./8.
g = 1./3.
mu = 0.001
k = 0.001
eps = 1.
g_b =0
l_b =0.1
c =1.

N = 1

#Initial state of infections(Random):
I0 = np.array([[random.randint(0,100)/100000.0 for x in xgrid] for y in ygrid])
S0 = np.ones((Nx+1,Ny+1))-I0
B0 = np.array([[0 for x in xgrid] for y in ygrid])

I0 = I0.flatten()
S0 = S0.flatten()
B0 = B0.flatten()

#Initial state of infections(Specific node):
I0 = np.zeros((Nx+1,Ny+1))
I0[int(Nx/2)][int(Ny/2)]=1
S0 = np.ones((Nx+1,Ny+1))-I0
B0 = np.array([[0 for x in xgrid] for y in ygrid])

I0 = I0.flatten()
S0 = S0.flatten()
B0 = B0.flatten()

#Non spatial function parts
def dS(S,I,B,N):
```

```
    return - B_h*I*S/N-B_e*(B/(B+c))*S - mu*S + k*N

def dI(S,I,B,N):
    return B_h*I*S/N-g*I+B_e*(B/(B+c))*S-mu*I

def dB(S,I,B,N):
    return eps*I-(l_b-g_b)*B

def Euler(dt,endtime,S0,I0,B0,N,A):
    S = S0
    I = I0
    B = B0
    for time in range(int(endtime/dt)):
        print(time*dt)
        Sc,Ic,Bc = np.copy(S),np.copy(I),np.copy(B)
        S = Sc + dt*dS(Sc,Ic,Bc,N) + dt*D_1*A*Sc
        I = Ic + dt*dI(Sc,Ic,Bc,N) + dt*D_2*A*Ic
        B = Bc + dt*dB(Sc,Ic,Bc,N) + dt*D_3*A*Bc
    return S,I,B
```